TECHNICAL UNIVERSITY OF CRETE
DEPARTMENT OF ELECTRICAL AND COMPUTER ENGINEERING

Masters Dissertation

Optimal Power Management and Control of Residential Microgrids

Προγραμματισμός Λειτουργίας και Έλεγχος Οικιακών Ενεργειακών Μικροδικτύων

Kalaitzakis Iason-Christos

EXAMINING COMMITTEE

Associate Professor Kanellos Fotios (Supervisor)

Associate Professor Koutroulis Eftychios

Professor Stavrakakis Georgios

Chania, August 2022

Acknowledgement

With many thanks to my supervisor, Prof. Kanellos Fotios for his assistance, support and guidance throughout the whole research project that resulted in this dissertation. I am also grateful to Prof. Koutroulis Eftychios and Prof. Stavrakakis Georgios for serving on my thesis committee and for their role in the research project.

I would also like to express my deepest appreciation and gratitude to my coworkers and friends Ioannis Roditis, Michail Dakanalis, Georgios Foteinopoulos and Ioannis Mandourarakis for their technical and moral support. Their presence in my life during these two years of my masters has been invaluable, with camaraderie and teamwork that will stay with me forever.

Finally, I would like to thank my parents, friends and family for their never-ending love and encouragement, with a special mention to my father since he inspired me to become an electrical engineer and has been supporting me every step of the way.

This dissertation was conducted as part of the research project ePOWER co-financed by the European Regional Development Fund of the European Union and Greek national funds through the Operational Program Competitiveness, Entrepreneurship and Innovation, under the call RESEARCH – CREATE – INNOVATE (project code: T2EDK-01775).

Abstract

The adoption of smart energy management systems at demand and distribution levels of the grid is mandated by the ever-increasing presence of smart grids. In this dissertation, a smart Home Energy Management System (HEMS) that reduces prosumers' daily energy costs and offers the grid ancillary services is proposed. Photovoltaic (PV) systems, Electric Vehicles (EV), Energy Storage Systems (ESS), flexible and critical loads, and a Multi-Port Converter (MPC) that connects the aforementioned modules with the power grid make up the residential prosumer residence. Optimal power management is carried out using the Particle Swarm Optimization (PSO) method. The HEMS also features the ability to function independently, by cutting its connection to the main grid. Additionally, the designed system can support grid frequency while taking into account the operational flexibility of the controlled power sources and loads. The use of k-means clustering and feed-forward neural networks in a load demand forecasting system is also proposed. The results obtained from the proposed system demonstrate that the HEMS minimizes the residential prosumer's operating costs, supports system frequency optimally, satisfies all operational requirements of the controlled system, and maintains the operational flexibility of all cooperating power components at the highest level.

Περίληψη

Η ραγδαία ανάπτυξη και διάχυση της τεχνολογίας Smart Grid στο ηλεκτρικό δίκτυο επέβαλε και την ανάγκη για πιο έξυπνα συστήματα διαχείρισης ενέργειας, τόσο στο επίπεδο μεταφοράς όσο και στο επίπεδο διανομής. Σε αυτή τη διατριβή μελετήθηκε, σχεδιάστηκε και αναπτύχθηκε ένα έξυπνο Οικιακό Σύστημα Διαχείρισης Ενέργειας (ΟΣΔΕ) το οποίο μειώνει το ημερήσιο ενεργειακό κόστος της οικίας και επιπρόσθετα προσφέρει βοηθητικές υπηρεσίες στο δίκτυο. Η έξυπνη οικία του καταναλωτή/παραγωγού θεωρείται ότι εμπεριέχει φωτοβολταϊκά πάνελ, ηλεκτρικό όχημα, συστήματα αποθήκευσης ενέργειας, ευέλικτα και κρίσιμα φορτία, καθώς και ένα μετατροπέα πολλαπλών θυρών ο οποίος διασυνδέει όλα τα παραπάνω με το κεντρικό ηλεκτρικό δίκτυο. Η βέλτιστη διαχείριση ενέργειας επιτυγχάνεται με τη χρήση του αλγορίθμου Particle Swarm Optimization - Βελτιστοποίηση Σμήνους Σωματιδίων. Το ΟΣΔΕ είναι επίσης σχεδιασμένο να λειτουργεί και αυτόνομα, δηλαδή χωρίς να είναι συνδεδεμένο με το κεντρικό δίκτυο. Η στήριξη συχνότητας του κεντρικού δικτύου εξασφαλίζεται βέλτιστα, λαμβάνοντας ταυτόχρονα υπόψη την ευελιξία ισχύος της κάθε μονάδας του συστήματος. Προτείνεται επίσης ο συνδυασμός των μεθόδων k-means clustering και feed-forward νευρωνικών δικτύων σε ένα σύστημα πρόβλεψης της κατανάλωσης ενέργειας από τα οικιακά φορτία. Τα αποτελέσματα που προέκυψαν από το προτεινόμενο ΟΣΔΕ αποδεικνύουν την αποτελεσματικότητα του συστήματος στην μείωση του ημερήσιου κόστους ηλεκτρικής ενέργειας, ενώ ταυτόχρονα τηρούνται και όλοι οι περιορισμοί που είναι εγγενείς στο παραπάνω σύστημα ισχύος.

Publications

- I. Kalaitzakis, M. Dakanalis and F. D. Kanellos, "Optimal Power Management for Residential PEV Chargers with Frequency Support Capability," *2021 10th International Conference on Modern Circuits and Systems Technologies (MOCAST)*, pp. 1-4, 2021.

- I. Kalaitzakis, M. Dakanalis and F. D. Kanellos, "Optimal Frequency Support by Residential Multi-Port Power Converters," *2022 11th International Conference on Modern Circuits and Systems Technologies (MOCAST)*, 2022, pp. 1-4, doi: 10.1109/MOCAST54814.2022.9837605.

- I. Kalaitzakis and F. D. Kanellos, " Optimal Energy Management and Control System for Multi-Source Smart Residential Prosumers," Submitted to *IEEE Transactions on Sustainable Energy*

Contents

1.
INTRODUCTION

1.1 General

Due to the ongoing energy crisis, conventional power generation has been ineffective in providing the necessary energy to the power grid. The cleaner, more environmentally friendly energy of Renewable Energy Sources (RES) has been in the foreground of research in the last few decades. To better exploit the energy of RES, ESSs are combined with RES to assist with their intermittency. Finally, optimal control of the demand side of the power equilibrium is also required in order to reduce energy demand. Due to the aforementioned trends, the modern power grids follow a decentralized architecture, with a big part of power generation carried out by the consumers. The decentralized power generation modules are called Distributed Energy Resources (DER) and they are located throughout the distribution network.

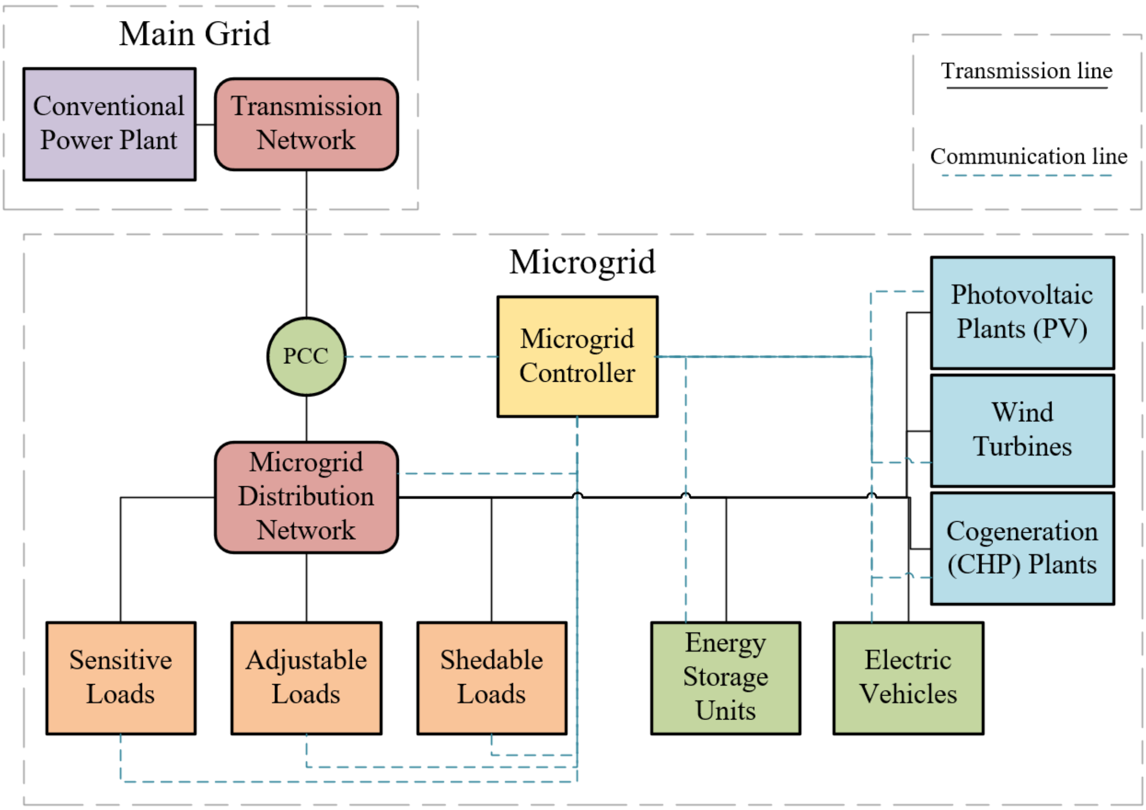

Fig. 1.1 – Microgrid topology.

Grid decentralization introduces new concerns to the grid, such as the bidirectional power flow required by DERs and ESSs, and the intermittency and low quality of power produced by RES. The solution for the aforementioned issues comes in the form of Microgrids (MG), which consist of DERs, ESSs and controllable loads [1]. MGs feature simpler power control due to their small scale, and also have the ability to disconnect from the main grid for extended periods and provide ancillary services. The general topology of MGs is seen in Fig. 1.1, as well as their power components and connection point with the main grid.

In residential-scale MGs, the most common DER is a rooftop installation of solar PV arrays. The energy produced by the PV arrays can be used to power local loads, saved in the ESS (if any are present) or sold to the grid if net metering or feed-in tariffs are provided by the power aggregator [2]. Additionally, due to the increasing popularity of EVs, it is worth examining them as a separate power module attached to the residential MG. Using the EV battery as an ESS is known as Vehicle-to-grid (V2G) [3], [4], a technology that will be explained more thoroughly in the following chapters.

The controllable loads of the prosumer can be shifted to different timeslots in order to better match the main grid and microgrid's needs for energy consumption. This process is called Demand Response (DR), and can be effective in balancing supply and demand without having to rely in the less dynamic supply-side management [5]. The combination of processors, controllers, communication infrastructure and actuators required to optimally manage the modules of a residential microgrid is referred to in literature as a Home Energy Management System (HEMS).

Since MGs connected to the main grid have the ability to both absorb and provide active and reactive power, they can also provide ancillary services to the main grid in order to support its power quality and stability. For the purpose of this dissertation, the provision of primary and secondary frequency support is researched and evaluated [6], [7]. This is because ESSs are able to absorb and provide power, and the demand side management can increase or decrease residential load demand, thus assisting in frequency support.

1.2 Related Work

Since the trend of grid decentralization shifted the focus of power management to the prosumer, HEMSs for residential microgrids are receiving increased research interest. The state-of-the-art surveys conducted by the authors of [8] and [9] analyze the aspects of HEMSs, such as their components, optimization technologies, performance metrics, setups but also the related issues and challenges.

The components in modern prosumer residences interact with each other, and their proper coordination is essential in the optimal operation of the HEMS. In [11], the residence comprises a PV and an ESS, and the optimization problem is solved using PSO. The research work presented in [12] incorporates model-based HVAC optimization, and in [13], a heat pump is included in the optimization of the building. The combination of EVs, ESSs and PV arrays is examined in [14]-[19], with varying focus on the components, user satisfaction and cost optimization.

The research work examined in this paragraph utilizes flexible loads to apply DR to the prosumer residence. In [20]-[22], DR and PV arrays are combined, and additionally an EV is included in [20] and an ESS in [21], [22]. More complex systems are examined in [23] and [24], with EVs, ESSs, PV arrays and flexible loads. A wind turbine is utilized in [25] instead of a PV array.

The aforementioned studies however lack the joint power management of all the mentioned power components prevalent in modern residences. This dissertation considers a residence that includes EVs, ESSs, PV arrays, flexible loads and thermal loads. Additionally, a thermal model of the residence is considered, and a novel load forecasting system is proposed.

Finally, the ability of a prosumer residence to provide frequency support is rarely mentioned in literature, with Lundstrom et al. [6] being a rare exception of a primary frequency support system that utilizes flexible loads and DERs. In this dissertation, the frequency support provided by the residential MG is optimized according to the flexibilities of the present power components, thus taking the provision of ancillary services a step further.

1.3 Contributions

In this dissertation, a multi-faceted HEMS is proposed, comprising an MPC, an EV, a home battery, a PV array, flexible residential loads and a connection to the power grid. The PSO algorithm is utilized to perform the day-ahead power management optimization, taking into account forecasts of temperature, energy price and solar irradiance, as well as following system constraints and user preferences.

The contributions of this dissertation are:

- The complex HEMS includes a variety of power components that are found in prosumer residences. The algorithm optimizes the power flows while following module constraints, user comfort, battery health, and convenience.

- The ancillary service of frequency support provided to the grid is combined with the maximization of component flexibility, using coefficients that accurately estimate the flexibility of the battery pack, the EV battery and the residential loads.

- The HEMS enables the microgrid to remain islanded for some period of time, while still using the stored energy optimally and avoiding the shedding of loads as much as possible.

- The residence is modelled using a thermodynamic model in order to fully utilize the optimization potential of the thermal loads of the residence. The HVAC system is able to maintain comfortable temperature levels while remaining optimal in its energy use.

- A novel electrical load forecasting method is proposed that combines fields of machine learning in order to reach an accurate estimation.

1.4 Dissertation outline

This dissertation is organized as it follows. Chapter 2 provides a general outline on microgrid related literature that will be useful in developing and implementing the system model. Chapter 3 describes the detailed model of the prosumer residence and its modules, the optimization framework and the provided ancillary services. The results of each simulated scenario of the HEMS are provided and analyzed in Chapter 4, as well as a general cost analysis. Finally, concluding remarks are given in Chapter 5.

2.
MICROGRIDS

Microgrids are defined as electrical grids that act as a single entity, and feature power sources, loads and (possibly) a connection to the main grid. Microgrids can scale from residential MGs that feature one residential prosumer, to entire residential or industrial blocks. The experimental part of this dissertation examines residential MGs, but the theoretical background analysis conducted in this chapter will cover subjects regarding all types of microgrids.

2.1 Distributed Generation

The power grid has been trending the past few decades towards the replacement of centralized generation with decentralized generation, also called Distributed Generation (DG). DG features DERs spread throughout the low voltage distribution network instead of just centralized power plants, as seen in Fig. 2.1. DERs produce energy for a higher cost (higher levelized cost of energy), but they come with a plethora of advantages over centralized generation:

- **Reduced power losses on transmission lines and transformers** - DER units are located closer to consumers, and thus feature reduced thermal losses on the transmission lines. Additionally, the produced power's voltage is closer or equal with the distribution network voltage, thus reducing conversion losses on step-down transformers.
- **Stability and grid robustness -** The failure of a DER would result in a manageable power loss on the power network, unlike the failure of a conventional power plant. Equally important is the comparatively smaller inertia of DER power sources, which allows them to adapt to the grid's needs more swiftly.
- **Environmentally friendly** - A significant percentage of DERs are RES, thus limiting their carbon footprint and allowing cleaner energy production.

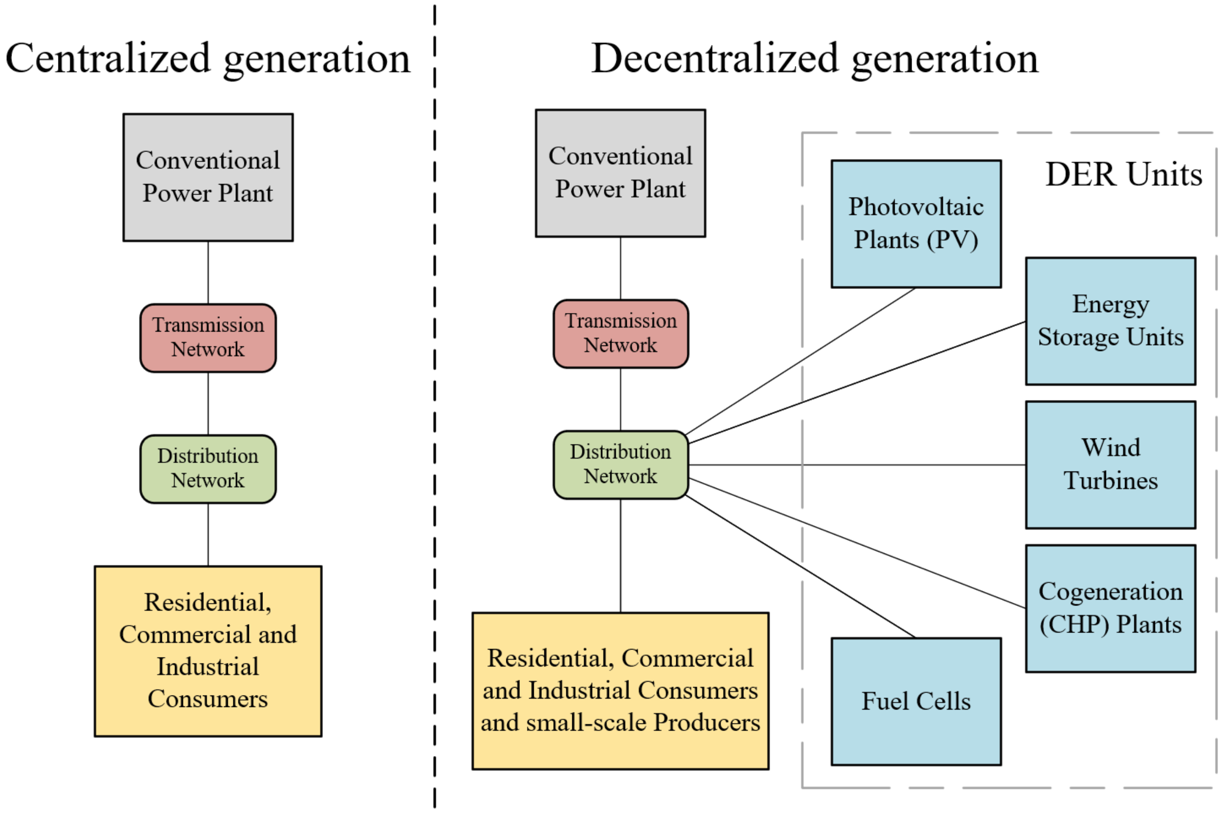

Fig. 2.1 – Centralized and Distributed Generation.

The DER units can be categorized depending on their type of interface with the grid, and the controllability of their power output.

Depending on their type of interface with the grid:

Rotary units – Rotary units are connected to the grid through a synchronized rotating generator. Such units can be reciprocating engines, small hydro and fixed-speed wind turbines.

Electronically coupled units – Units electronically coupled with the grid through power converters. Examples of such units are variable-speed wind turbines, PV panels, fuel cells.

Depending on the controllability of their power output:

Dispatchable unit – Dispatchable units can adjust their power output in a relatively short time window. These units usually consume fuel, such as reciprocating engines and fuel cells.

Non-dispatchable unit – Non-dispatchable units have their power output tied to external factors, usually depending on the operating condition of their primary energy source (common with RES). Examples of such units are PV arrays, wind turbines, hydroelectric stations.

2.2 Power Generation

The aforementioned DER units are responsible for the power generation that is carried out in MGs. This subchapter lists the most common power sources found in MGs.

2.2.1 PV Arrays

PV Arrays utilize the photovoltaic effect of semiconductors to produce electricity from the solar energy of sun rays. They are a swiftly evolving renewable source, and highly popular the last two decades, since the price (€/watt) of solar panels has dropped significantly. Their popularity is also attributed to their scalability, since they can range from a simple rooftop installation to a complex solar farm spanning over many acres.

Additionally, PV arrays are environmentally friendly, noise-free and of low maintenance. The forecast of power production of solar panels is relatively accurate through modelling and weather forecasts regarding temperature, solar irradiance, cloud coverage, humidity and wind speed. The efficiency of power conversion from solar to electrical energy is currently around 15-20%, but more efficient cells are still being invented.

Like all RES, PV Arrays are frequency combined with ESSs, such as battery packs. An ESS can absorb and store the excess of power generated by PVs at noon, and inject it to the microgrid during a period of low PV production.

2.2.2 Internal Combustion Engine

Internal Combustion Engines (ICE) are heat engines which exploit the high temperature and high-pressure gasses of combustion to generate force on a piston or a rotor and produce electricity. Most commonly found in MGs as Diesel or Gas engines, they can be used as a constant power supply or an emergency power source in case of issues with the main grid. Microturbines are also common ICEs, but they instead utilize the force of the combustion on a turbine (instead of on a piston) to produce electricity.

ICEs are not environmentally friendly, as they use fossil fuels to operate Their main advantage is their dispatchability. However, there are types of ICEs that use renewable fuels, such as biodiesel, bioethanol or hydrogen.

Diesel engines (portable generators) are frequently utilized as a backup for residential-scale microgrids in the event of a grid failure that causes the microgrid to become disconnected from the main grid. The diesel engine has a high energy density, cheap fuel costs, and low maintenance needs, all of which make it an effective backup system.

2.2.3 Hydrogen Fuel Cells

Hydrogen fuel cells utilize the electrical energy created through the redox reaction of Hydrogen and Oxygen.

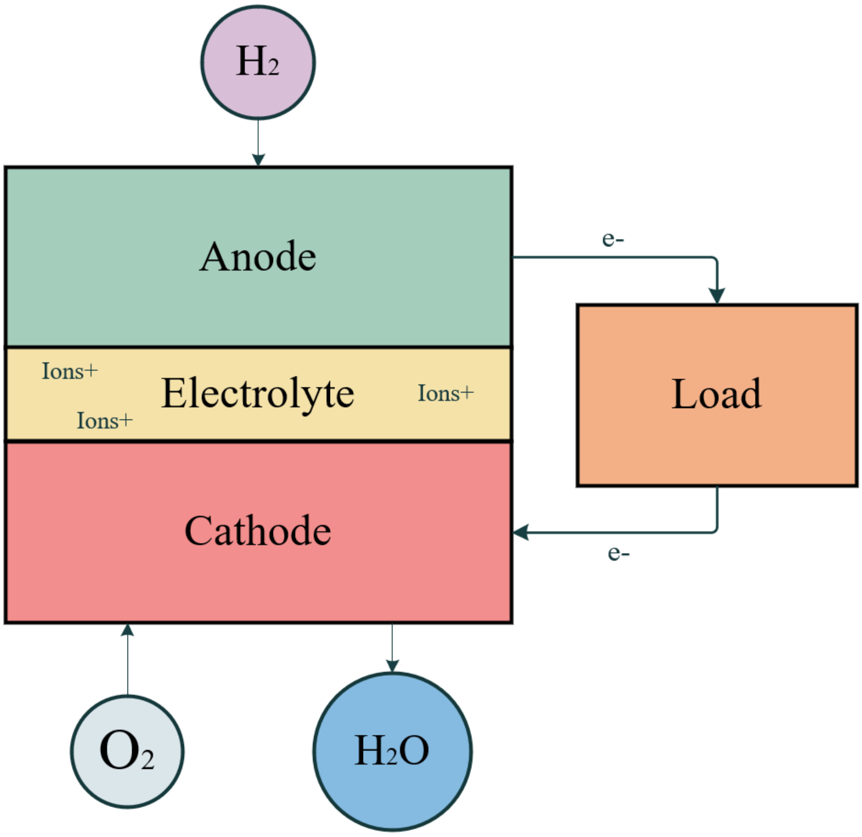

Fig. 2.2 – Hydrogen Fuel Cell Design.

Just like ICEs, fuel cells convert chemical energy to electrical energy, but their only waste product is water. The aforementioned fact, together with the method of electrolyzing water to produce hydrogen, makes fuel cells substantially more ecologically friendly.

Due to their low weight, compact setup, constant power availability and lack of moving parts, fuel cells are reliable standalone power sources to islanded microgrids. Additionally, they feature a significantly high 40-60% energy efficiency, compared to the 25% of ICEs. However, the necessary equipment to utilize fuel cells is both and expensive and difficult in its installation, requiring more specialized personnel. Residential fuel cell use is not very common, but this could change in the future.

2.2.4 Combined Heat Power - Cogeneration/Trigeneration

Combined Heat Power (CHP) or Cogeneration is the utilization of the heat byproduct of heat engines or power stations for heating. This reduction in thermal losses increases the efficiency of power production. Although they are a relatively new innovation in DER systems, micro-CHP units have already shown to be an extremely useful technology in lowering the carbon footprint of non-renewable fuels.

Next to Cogeneration is Trigeneration technology, the concept of utilizing heat engines of power stations for electricity, heating and cooling. Trigeneration is similar to cogeneration, except for the fact that medium-scale heat (100-180ºC) is instead used by absorption chillers for cooling.

2.2.5 Wind Turbines

Through the use of generators, wind turbines transform the kinetic energy of the wind into electrical energy (the wind’s power rotates blades attached to the rotor to produce electricity).

Wind turbines are not as scalable as PVs, and thus are not as common in MGs. Most wind turbines require a large amount of free space and have high capital costs, which makes them more ideal for large scale projects. However, there exist residential scale wind turbines, such as the Gorlov-type helical wind turbine, which can be installed in building roofs.

2.2.6 Hybrid Renewable Energy Systems

There are many well-known disadvantages in RES that need to be considered before their diffusion in MGs or the main grid. Power production localized in specific time periods, production stochasticity and other instability issues can be solved by combining different types of RES systems together. That is the essence of Hybrid RES installations.

Examples of these hybrid systems are PV arrays and wind turbines combined together, since their peak power outputs are usually on different hours of the day. Numerous combinations can be made from just solar, wind, biomass and hydrogen plants, with the latter two not having time-of-the-day restrictions. A Hybrid RES system combined with an energy storage system can provide even greater energy balance and system efficiency.

2.3 Load Management

A basic concept of operation of a microgrid is the balance of supply and demand in power. Lack of balance in this equilibrium can be fixed by adjusting the power consumption from the main grid, assuming the MG is not islanded. However, the supply side of the equilibrium is both slower in its response, and more expensive to adjust. Conventional generators require downtime before they can be started again and uptime before they can be shut off, as well as some time to alter their power output. For this reason, it is economically beneficial to instead adjust the demand side, aka the electric loads. Depending on their ability to be adjusted/shifted, all loads, from residential to industrial can be categorized as follows:

- **Critical Loads**

The devices/machines that cannot afford any disruption to their operation are classified as critical loads. This inflexibility can be attributed to economic (industrial/commercial loads), medical (healthcare buildings) or quality of life reasons (personal computers, TVs). Only in the direst of circumstances can these loads be shed, in order to avoid a total blackout.

- **Adjustable Loads**

Adjustable loads are the devices that have controllable output levels, and thus can alternate their power consumption to match the grid’s needs without affecting the end result as much as a binary power state would. Examples of such loads are dimmable lights, and HVAC systems.

HVAC systems more specifically are very important demand response candidates, since they are usually around half of the power consumption of a residence, and the inertia of heat can assist in peak shaving if planned around optimally.

- **Shiftable Loads**

All loads that can be time-shifted into different time slots of the day are classified as shiftable. Shiftable loads are the most flexible to plan around in the demand response management of a MG.

Washing machines, dryers, water heaters, and electric ovens are considered shiftable appliances since they may be turned on and off to reduce their consumption during periods of high demand. Electric vehicles belong in both the shiftable and adjustable categories, since, as it will be explained more thoroughly in a following subchapter, the charging operation can be both interrupted or adjusted in its power consumption.

2.3.1 Demand response

Demand Response (DR) management is the direct or indirect adjustment of the electrical loads to better match the demand for power with the supply. There are several methods to approach this adjustment:

Tariffs – Two-rate or off-peak tariffs are provided by many power aggregators to encourage consumers to schedule their power consumption during less busy time slots (usually provided as a day and night rate). It is the least invasive method of DR, enforced only by the economic incentive of shifting the flexible loads away from peak demand time slots.

Through the use of smart meters that are seeing increased penetration in modern power grids, a fully variable tariff with live updates can be the next step of DR. Since smart metered residences are equipped with an In-Home Display (IHD), the consumer can receive live information on the price of energy and adjust their loads accordingly.

Agreements – Power aggregators make agreements in their contacts, mostly with high-end industrial or commercial users. These agreements may force the aforementioned consumers to reduce their power consumption during peak demand, so as not to overburden the grid.

Targeted Blackouts – Targeted blackouts are a last resort solution in order to avoid a total blackout. The MG operator can decide to shut down components of the microgrid, such as residences, EV parking lots or industrial consumers.

This procedure is often applied to the Cretan power grid during the hottest days of summer, since the increased demand from tourism infrastructure and HVACs overwhelms the grid's energy production ability

2.4 Energy Storage

Energy storage systems comprise the devices or mechanisms that can be used to store energy in non-electric form (except capacitors) that can be later converted to electricity with relatively low losses.

The advantages of including energy storage in any modern macro power system have placed the sector in the foreground of research. Some of these benefits include:

- **Support for renewable energy**

Due to the intermittency and stochasticity of the power production of RES, most modern RES installations are paired with an ESS. The ESS can absorb excess power produced during optimal conditions (differs for each RES) and inject it back into the grid during peak demand/low RES production.

- **Voltage and Frequency support**

The energy stored in ESSs can be used to support the voltage or frequency of the microgrid. The ESS therefore assists in the power quality of the microgrid, and in the mitigation of possible faults.

- **Islanded Microgrid support**

The microgrids that are permanently or temporarily disconnected from the main grid require either a fully dispatchable and reliable power generation source, or ESSs. By using ESSs, the energy produced by RES sources can be saved and dispatched more evenly throughout the day. Additionally, islands microgrids require support in power quality, since the lack of connection to the main grid brings about power instability due to sudden load changes or RES power output drops.

The following subchapters list the most common ESSs used in microgrids:

2.4.1 Rechargeable Batteries

Batteries are devices that generate electricity through redox reactions using high-energy chemical reactants. They can be classified into primary (no recharging) and secondary/rechargeable. To be considered a proper ESS, a battery pack has to be rechargeable, and thus from now on in this dissertation the term battery will indicate the rechargeable version.

Electric batteries are by far the most widespread method of electrical energy storage, since they are efficient and flexible. They are also incredibly scaleable, ranging from powering a small device to a whole residence or EV. However, electric batteries are among the most expensive energy storage options when measured in terms of € to Wh. The price of the most popular battery types has been improving throughout the years, however, making residence-scale battery packs more affordable to the common consumer.

For the majority of battery types, proper control is necessary to maintain battery health. More specifically, each battery requires specific charging and discharging procedures in order to not reach the charging limits often, and temperature control, since high and low temperatures can damage battery health.

Different combinations of the electrodes and electrolytes used in batteries provide a variety of different battery types, each with its own special traits (Fig. 2.3).

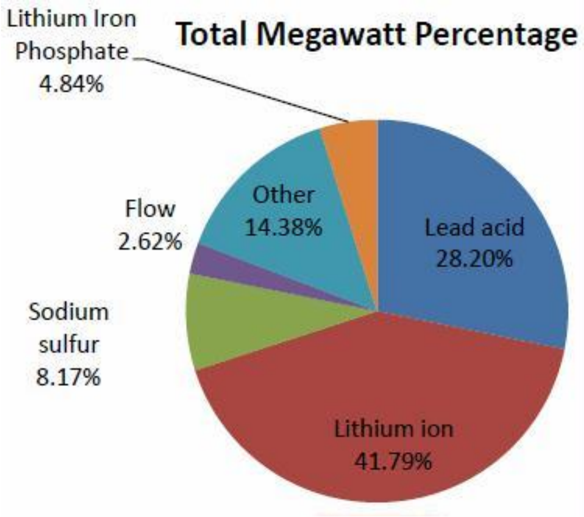

Fig. 2.3 – Percentage of Battery storage systems deployed in the U.S. by 2019. Source

The most common battery types are listed in the following paragraphs:

- **Lithium-Ion**

Since their emergence in the 1990s, Li-on batteries have become the most popular type of rechargeable battery in modern systems. Their use ranges from laptops, electric vehicles, cell phones, home battery packs and many more. The high energy density to weight ratio of Li-on batteries sets them as the frontrunners for microgrid energy storage applications, but they also feature little loss of charge and lack the memory effect found in other types of batteries. Disadvantages of Li-on batteries are the relatively high cost, and high temperature during operation. Lithium-ion Polymer batteries are a recent advancement in lithium-ion technology that enhance energy density and form flexibility.

- **Lead-Acid**

Lead acid batteries, the earliest rechargeable battery technology, are mostly used in automobiles. Because they are a well-established technology that is affordable and capable of producing large surge currents, they are frequently used in conjunction with starter motors and combustion engines. Similar to lithium-ion, they don't have a memory effect. However, lead-acid batteries are notorious for having a limited cycling capability, necessitating regular replacement and making them unfavorable for microgrid applications. Furthermore, a microgrid's goal is also to be environmentally friendly, and this battery's heavy metal components present a significant problem to that end.

- **Flow Batteries**

Flow batteries work by exploiting the ion exchange of two chemical components in two tanks that are separated by a membrane. Since the two fuel tanks may be refilled, they function similarly to fuel cells. This property eliminates the aging effect on flow batteries, giving them an advantage over the competition of Li-on and lead acid batteries. Since the battery pack of a microgrid can be stationary, flow batteries are a great solution in avoiding battery replacement costs.

2.4.2 Superpacitors

Supercapacitors (or ultracapacitors) (SC) are devices that store electrical energy in an electric field. They feature much higher capacity than the common capacitors found in small circuits. The difference of SCs and batteries is that SCs possess significantly higher power discharge rates and lifecycles, at the cost of less energy density. Because of this ability to swiftly discharge power into the grid or absorb power from the grid, ultracapacitors make for excellent balancing support units.

Supercapacitors are rarely installed as stand-alone units. They are usually combined with electric battery systems to form Hybrid Energy Storage Systems (HESS). In this combined HESS, the batteries aid with long-term power deficiencies while the capacitors offer short-term support.

2.4.3 Hydrogen Fuel Cells

The power generation part of hydrogen fuel cells has been analyzed in Chapter 2.2.3. They can also be classified as an ESS, however, due to the process known as electrolysis. By using DC current to electrolyze the water byproduct of fuel cells, the hydrogen can be reclaimed and reused at a later time. Therefore, similar to batteries, they can be utilized as electrochemical energy storage systems. The round-trip efficiency of a fuel cell ESS is about 40%, but it can be increased to 80% if combined with a CHP system mentioned in Chapter 2.2.4.

2.4.4 Pumped Hydroelectric Energy Storage

Pumped Hydroelectric Energy Storage (PHES) features two water reservoirs at different altitudes, connected through pumps and power generating turbines. The facility receives excess power to run the pumps and move water from the lower to the upper reservoir during periods of low demand. Water is then dropped via the turbines to generate power when the grid experiences high demand.

With a fantastic round-trip efficiency of 80%, hydroelectric energy storage outperforms most other energy storage technologies. Due to the great energy capacity, it accounts for more than 90% of the installed ESSs measured in rater power in the US (Fig. 2.4).

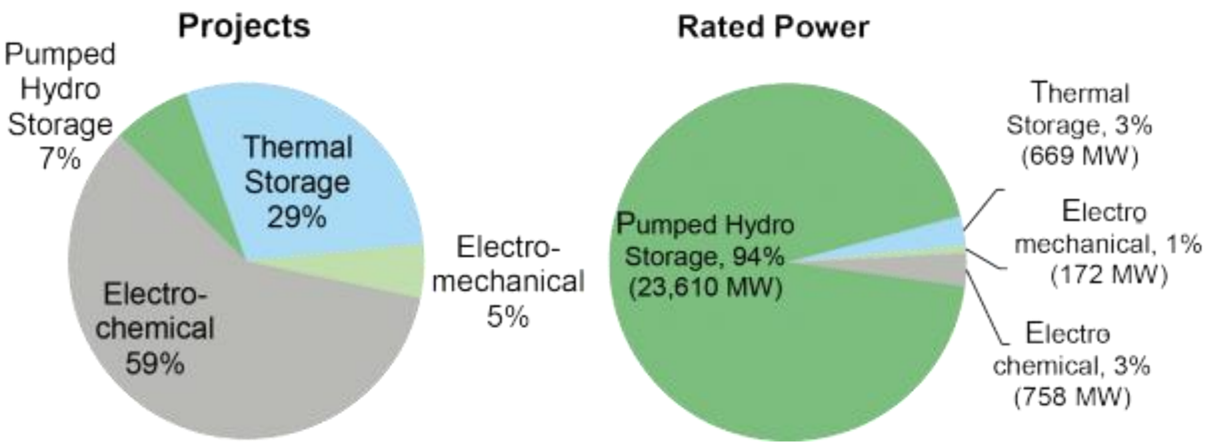

Fig. 2.4 – U.S. Energy storage Projects compared to their Rated Power, 2018. Source

However, the scale of PHES is larger than the energy storage needs of microgrids, with a very high initial investment cost. Thus, pumped hydro is still proof of concept in microgrids.

2.5 Electric Vehicles

It is widely known by now that EVs are the long-term more sustainable and economic solution as a private transportation method compared to conventional vehicles, especially due to the recent price hikes of liquid fuel. Many countries around the world have set future quotas for the penetration of EVs in their vehicle industry, and a few have banned the production of conventional vehicles altogether. In this dissertation, EVs are examined as a separate entity despite their utilization as ESSs and/or flexible loads, due to the complexity of their operation.

Some of the advantages of EVs over conventional vehicles are listed below:

- **Economic efficiency** – The cost-per-mile of electric motors is lower compared to the cost-per-mile of conventional engines, and the cost of electricity is usually affected less by market fluctuations. EVs also include fewer moving parts in their operation, and are therefore cheaper to maintain and have less breakdowns.

- **Limited air pollution** – The microparticles created by tire friction is the only air pollution actively produced by the usage of EVs. The passive EV air pollution, through the generation of the power they consume, is still lower compared to conventional vehicles. This is because RESs and other power sources that are more environmentally friendly than combustion engines are responsible for a significant percentage of energy generation in modern power grids.

- **Limited noise pollution** – The operation of electric motors produces noise that is many dBs lower than that of conventional engines. This fact is very important to modern cities that are facing severe noise pollution issues due to the ever-increasing number of vehicles.

The term Electric Vehicle includes different categories of automobiles that contain a battery and an electric motor. However, there is another step in their categorization, as seen in Fig. 2.5 and explained below:

- **Battery Electric Vehicles (BEV)**

Battery EVs contain an electric motor on which they rely entirely for acceleration of the vehicle. They also include a high-capacity battery that can be recharged through the power grid. Due to the high capacity of the battery, the microgrid prosumer will benefit most from the optimization method of the following chapters if the residential microgrid features a BEV.

- **Hybrid Electric Vehicles (HEV)**

Hybrid EVs include both an ICE and an electric motor. The electric motor, when not responsible for accelerating the vehicle, is used as a generator that charges the battery through the movement of the vehicle. HEVs usually operate with the electric motor in slow-traffic environments such as cities, and then switch to the ICE for high-speed areas such as highways. This is because the electric motor is more efficient with sudden speed deviations (traffic), and has higher acceleration speed, while the ICE is more efficient with maintaining high velocities.

HEV batteries cannot be interfaced with externally, and are usually of lower max capacity compared to other types of EVs. Thus, HEVs are not compatible with the model of this dissertation.

- **Plug-In Hybrid Electric Vehicles (PHEV)**

Plug-In Hybrid EVs are similar to HEVs, with a few key differences: a) the battery can be recharged through the power grid and b) the battery has higher capacity than that of HEVs. PHEVs can utilize the best of both worlds between electric motors and conventional engines, with the ability to rely solely on either one for extended periods of time.

However, their battery capacity is still a fraction of that of BEVs, establishing their use as grid energy storage systems as circumstantial.

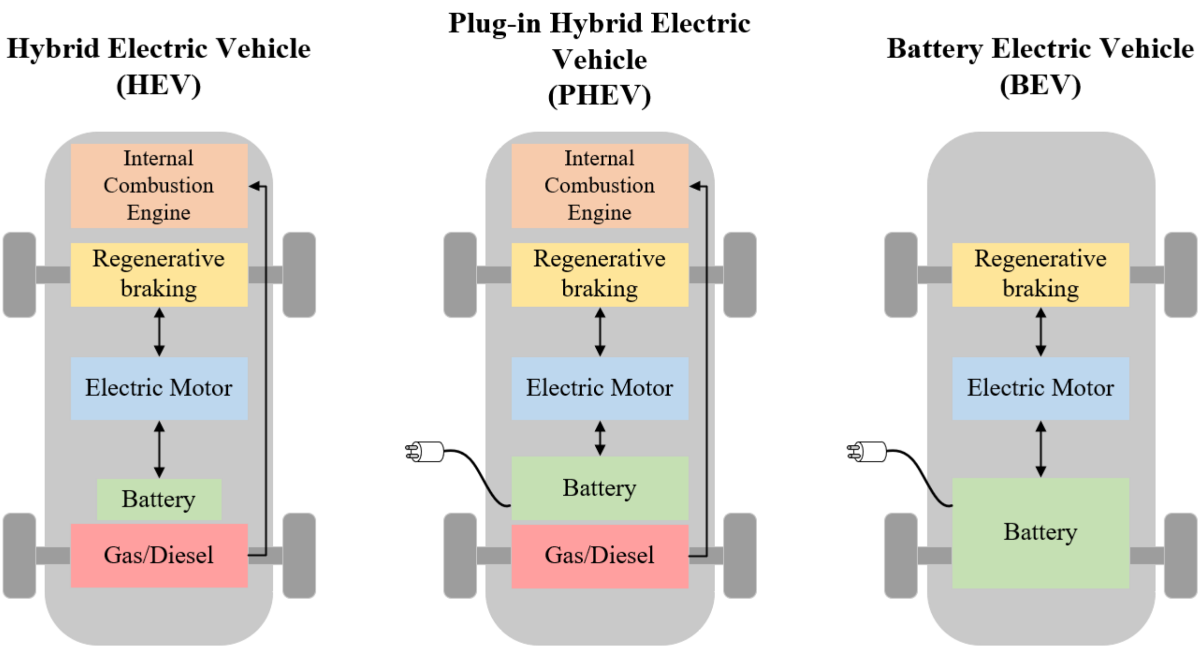

Fig. 2.5 – Comparison between different types of electric vehicles.

2.5.1 Battery charging methods

There are multiple charging methods for EV batteries connected to the grid, with most of them requiring specific equipment. This categorization depends on the capabilities of the battery itself, the connection point and the cables, and is explained below:

- **AC Charging**

The AC socket exists in all residences as the most basic battery charging method, and can provide around 1-3kW of power to the battery. While this is a cheap and accessible way to charge the EV battery, the low wattage necessitates for the EV to remain stationary for many hours while charging. Households with a three-phase power installation can reach up to 22kW of charging power when using all three phases, but these installations are not common.

More specialized single-phase sockets with dedicated circuit lines can reach up to 7kW, while protecting both the EV and the other household appliances. Additionally, these connectors offer load shedding functionality for a more efficient charging schedule.

- **DC Charging**

DC charging, also called DC Fast Charging, requires the use of an external AC-DC converter to provide the battery with DC current. This bypasses the need for an AC-DC converter inside the EV, which is usually the component that bottlenecks the charging process. By rectifying the AC current to DC with an external converter, DC charging in specialized charging locations and EV parking lots can reach power ratings of 50-350kW, charging the EV battery in minutes. The power electronics of the converter include all the control and protection utilities required.

2.5.1 Vehicle to Grid

For a microgrid, the spread of EVs throughout the grid can present challenges as well as opportunities. Sudden increased power demand is the major issue brought on by the rapid development of EVs, since it is another load that did not exist for the equivalent conventional vehicle. If the rate of growing demand is not met by an equally increasing power production, unprepared power grids will have to face a severe energy crisis.

The utilization of EV batteries in assisting the main grid and microgrids is based on the following facts:

1. The average EV remains parked for the majority of the day, either at the residence or a workplace/commercial parking lot. Consequently, the battery is available to the grid for the most of the day.

2. The power flow of modern chargers, as seen in Chapter 2.5.1, can charge/discharge the battery from full to empty and vice versa in a few hours for AC, and minutes for DC current.

3. The battery of a BEV has enough capacity to power an entire residence for a day or more.

By considering the above facts, it can be concluded that EV batteries can be utilized as flexible loads or as ESSs by the grid they are connected to. This technology is called Vehicle-to-grid (V2G), and it can be categorized into two main models:

- **Unidirectional V2G (V1G)**

Unidirectional V2G (V1G) is defined as the controlled charging of the EV battery, also referred to in literature as Smart Charging. In V1G, the aggregator responsible for charging the EV battery is able to alter the power flow to the vehicle, either throttling it or stopping it entirely. If information on the vehicle's departure time is provided, the charging process can be optimized to assist the microgrid with peak shaving and valley filling. Additionally, a smart microgrid with a holistic day-ahead power management system can apply this information to achieve peak RES utilization.

In other words, the V1G method handles the EV as a flexible load with the constraint of a departure time. Compared to bidirectional V2G, V1G is the less invasive, easier to implement technique with proven cost effectiveness. While V1G does have the drawbacks that V2G is criticized for, it also cannot achieve the maximum cost saving that V2G can.

- **Bidirectional V2G**

Bidirectional V2G is defined as the system that utilizes the EV battery as an ESS, allowing it to both charge/discharge energy from/to the grid or microgrid. As long as this operation does not disturb the requirement for the battery to be full by departure time, the aggregator can use the stored energy during peak demand and return it during low demand. Additionally, the EV battery can be used for voltage and frequency support.

The V2G technology, while it can be utilized for increased economic benefit, is a controversial method in the EV scientific community. The battery of an EV is usually a third of the total cost of the vehicle, and, as it was mentioned in Chapter 2.4.1, each battery has limited cycles before degradation reduces its capacity to a point where it has to be replaced. EV owners are therefore reluctant to allow V2G to reduce the battery's lifespan. Studies on the subject have yielded different results, with some proving that the battery aging nullifies any economic benefit [30],[31], and other concluding that V2G can actually increase battery life [32]. Additionally, it is not proven whether V2G is economically viable as a technology, considering that cost of batteries and losses due to low round-trip efficiency can negate any economic benefits [45]. It should be noted however that the cost of batteries has been decreasing, which is a promising trend on the viability of V2G.

.

3.
System Modelling

In this chapter, a rundown of the simulated prosumer residence is provided. The models developed and implemented for each power component are analyzed, as well as the general optimization algorithm for the power management performed by the HEMS.

3.1 Model Description

In Fig. 3.1, the structure of the examined home prosumer, as well as the suggested energy management and control system is depicted. The prosumer residence consists of the following modules: an EV, a home battery pack, a PV system, and a combination of flexible and critical electrical loads, as well as heating/cooling loads. The aforementioned modules connect and interact with each other and the grid through an MPC, which in turn interfaces with the grid through a PCC. The MPC, the PCC and the aforementioned power modules are all controlled by the proposed HEMS, the system that is the focus of this dissertation. Additionally, in order to achieve optimal power management of the residence, the proposed system features external streams of information/forecasts. These inputs comprise forecasts from the electric power system operator and the local meteorological service and information from the user of the HEMS.

The PSO algorithm is utilized for the day-ahead power optimization. This method requires both user input and external data as inputs. Such inputs include power module technical characteristics, EV activity schedule, EV driver preferences (final energy target, charging cycle limitation), forecasts of environment temperature, solar irradiance, residence load, and electricity price, and the technical characteristics and parameters of the residential thermal system.

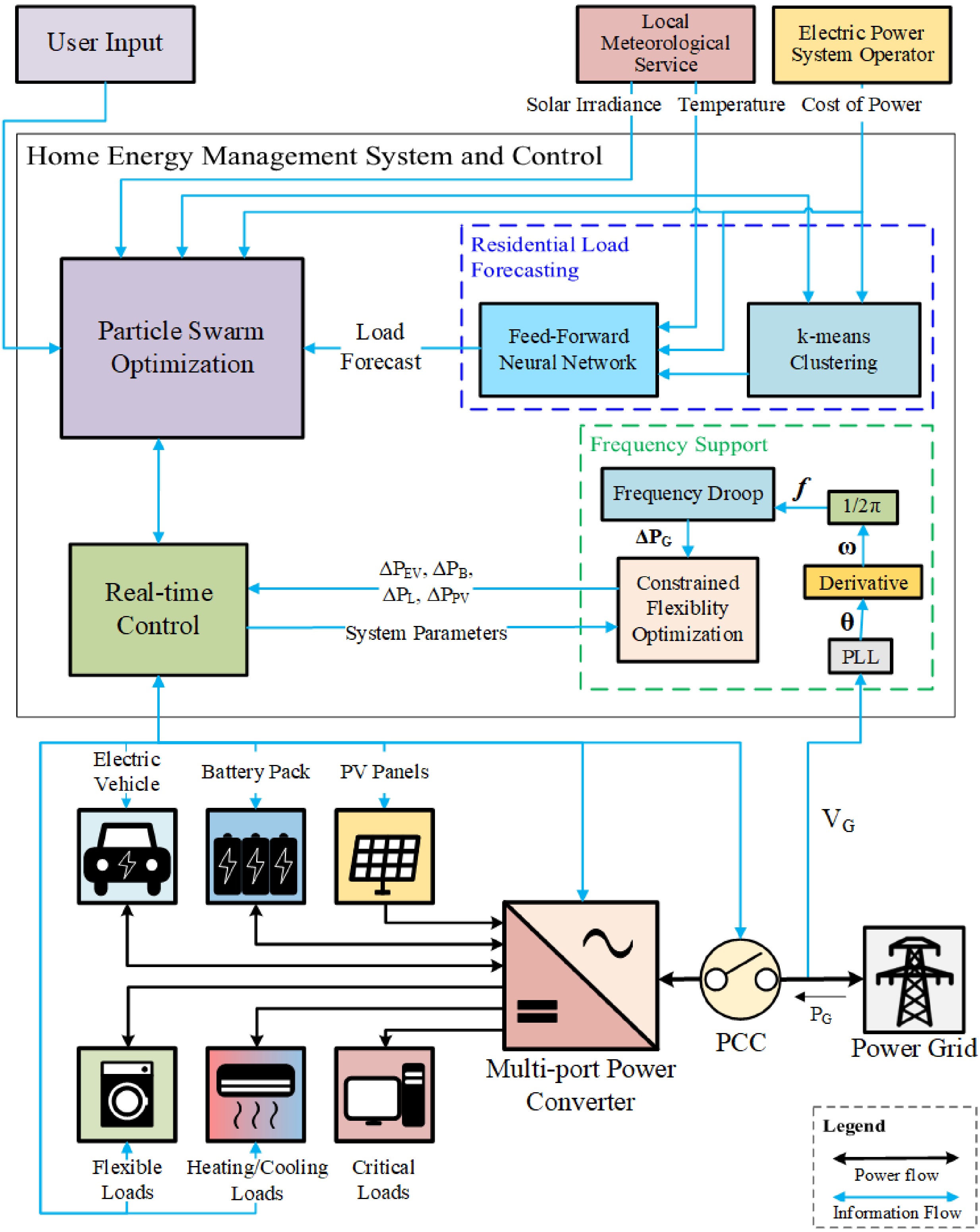

Fig. 3.1 – Block diagram of the EMS and the MPC configuration.

Moving on to the residential electric load forecasting system, its inputs consist of forecasts of the electricity price and environment temperature. The residential load forecast system is assisted with the use of a typical load profile obtained by the clustering of previous temperature, electricity price and residential load daily profiles. The final step of the load forecasting method is the use of a feed-forward Artificial Neural Network (ANN) with inputs from the aforementioned clustering method, temperature and cost of power forecasts to provide a load forecast. This load forecast is then provided to the optimization algorithm for the day-ahead optimization.

Finally, at the bottom right of the HEMS module, the frequency support system can be seen. In order to provide frequency support, first the grid's frequency is measured using the PLL method. If the grid frequency deviates outside of a predetermined dead-band of the droop characteristic, the frequency support system is activated. The system's current state and parameters are taken into account as a new power management trajectory is calculated by the flexibility optimization method, bypassing the original optimal power trajectory and setting new set-points to the real-time control system of the MPC. In this way, the residence provides frequency support to the grid while also maintaining the highest possible flexibility for its modules.

The specifics of each HEMS block shown in Fig. 3.1 and briefly analyzed above will be explained more thoroughly in the following subchapters.

3.2 Battery Modelling

The EV battery and the home battery are modelled mathematically, following the constraints and formulas listed in this subchapter. In (1), the maximum and minimum power rate of the batteries is formulized, and the maximum and minimum energy levels are shown in (2). Equation (2) also shows how the energy level of the batteries is calculated at each point in time. In constraint (3), the HEMS is forced to charge the EV battery above a predetermined level before the EV begins its trip. The energy level of the battery at the end of the day-ahead optimization is dictated by (4), as set by the residential microgrid operator, and constraint (5) limits the charging cycles. By limiting charging cycles, the user can reduce the invasiveness of the algorithm and increase battery life, at the cost of lower economic benefit from power management.

$$P_{B(EV),min} \leq P_{B(EV)}(t) \leq P_{B(EV),max} \; \forall t \tag{1}$$

$$E_{B(EV),min} \leq E_{B(EV)}(0) + \sum_{0:dt:t} \left(P_{B(EV)}(t) \cdot dt\right) \leq E_{B(EV),max} \; \forall t \tag{2}$$

$$E_{EV}(0) + \sum_{t=0:dt:t_d} (P_{EV}(t) \cdot dt) \geq E_d \tag{3}$$

$$E_{B(EV)}(0) + \sum_{t=0:dt:T} \left(P_{B(EV)}(t) \cdot dt\right) = E_{B(EV)}(T) \tag{4}$$

$$Charging\_cycles\_count \left(\int P_{B(EV)} \cdot dt \right) \leq N_c \tag{5}$$

where $P_{B(EV)}$ (kW) is the home (EV) battery charging/discharging rate following load convention, $P_{B(EV),\mathrm{max(min)}}$ (kW) is the home (EV) battery maximum (minimum) charging rate. $E_{B(EV),max}$ and $E_{B(EV),min}$ (kWh) are the maximum and minimum energy levels stored in home (EV) battery. N_c is the maximum number of allowed charging cycles as defined by the HEMS operator.

An additional measure to preserve battery health and prevent aging is taken through constraint (2). The $E_{B(EV),min}$ and $E_{B(EV),max}$ values are set to 10% and 90% of the battery's rated capacity respectively, as it is proven that overcharging or fully depleting a battery accelerates its aging process.

3.3 Thermodynamic Modelling

It is a fact that HVAC systems are a very important load of each residence, as they can account to approximately half of the electricity usage of the average modern prosumer. Additionally, thermal energy features inertia that is multitudes higher than that of electrical energy, a behavior that can be utilized by the HEMS to optimize the heating/cooling system's energy cost. Due to the two aforementioned facts, the HEMS proposed in this dissertation includes the thermal modelling of the residence, with thorough heat transfer formulas as presented by [26] and [27]. The thermal modelling of the residence is formulized as follows:

$$\rho \cdot C \cdot \mathrm{V} \cdot \frac{dT_{in}(t)}{dt} = \dot{Q}_{wall}(t) + \dot{Q}_{win}(t) + \dot{Q}_{in}(t) + \dot{Q}_{sw}(t) + \dot{Q}_{sg}(t) - \dot{Q}_{EC}(t) \tag{6}$$

$$\dot{Q}_{wall} = U_{wall} \cdot F_{wall} \cdot (T_{out} - T_{in}) \tag{7}$$

$$\dot{Q}_{win} = U_{win} \cdot F_{win} \cdot (T_{out} - T_{in}) \tag{8}$$

$$\dot{Q}_{sw} = \alpha_w \cdot R_{sej} \cdot U_{wall} \cdot F_{wall} \cdot I_T \tag{9}$$

$$\dot{Q}_{sg} = t_{win} \cdot SC \cdot F_{win} \cdot I_T \tag{10}$$

$$\dot{Q}_{EC}(t) = P_{EC}(t) \cdot COP \tag{11}$$

where ρ is the air density, C is the thermal capacity of the air, V is the air volume of the residence and T_{in} is the indoor temperature. $\dot{Q}$ is the transfer of heat energy. More specifically, $\dot{Q}_{in}$ denotes the internal heat gains (heat generated by human activity, devices etc.) and $\dot{Q}_{sw}$, $\dot{Q}_{sg}$ the heat contributions due to solar radiation on walls and windows, respectively. U_{wall} and U_{win} are the heat transfer coefficients of the walls and windows, and F_{wall} and F_{win} are the areas of walls (including the roof) and windows, respectively. T_{out} is the outdoor temperature, α_w is the absorbance coefficient of the external wall surface, R_{sej} is the external surface heat resistance, t_{win} is the glass transmission coefficient of the windows and SC is the shading coefficient of the windows. Finally, I_T is the solar radiation absorbed by a tilted surface in [28].

The main thermal formula of (6) features the relationship between the indoor temperature T_{in} and the power consumption of the HVAC, $\dot{Q}_{EC}(t)$. The rest of the equations detail the heat energy transfer that happens naturally in the residence. More specifically, (7) is the heat transfer between outer and inner walls, (8) is the heat transfer through windows, (9) is the solar energy converted to heat through the walls, and (10) is the solar energy converted to heat through the windows.

The conversion between the electrical energy consumed by the HVAC and the thermal output of that energy is shown in (11). The coefficient COP, known as Coefficient Of Performance, is the rate with which electrical energy is converted to thermal, and it depends on the quality of the HVAC system.

3.4 Residential Electric Load Forecasting

The forecast of the residence's electric load is required by the HEMS in order to properly predict the energy exchange between the residential microgrid and the grid. A residential load forecasting system is therefore proposed in this dissertation, consisting of two distinct prediction methods combined to create a more efficient load forecasting approach. The two proposed methods are the k-means clustering algorithm and an ANN. The HVAC load is already approximated by the PSO algorithm and therefore not part of the residential load forecasting process.

It should be noted that the daily power consumption of a residence follows difficult to predict, stochastic patterns due to the human element in its nature.

The dataset of residential loads used as input in the clustering algorithm was created by accurately modelling each device of a residence, with behavioral profiles depending on the employment status and shift of the main resident as well as the current season. Additionally, some stochasticity was added to the time of use and power consumption of each appliance, to account for the human element that is present in all load profiles. The above loads are superimposed to a residential base load pattern.

The proposed load forecasting system's topology is depicted in Fig. 3.2. EP(t) and Tout(t) represent the electricity price and outdoor temperature respectively. The time series of temperature and electricity price forecasts were taken from real databases for the city of Chania.

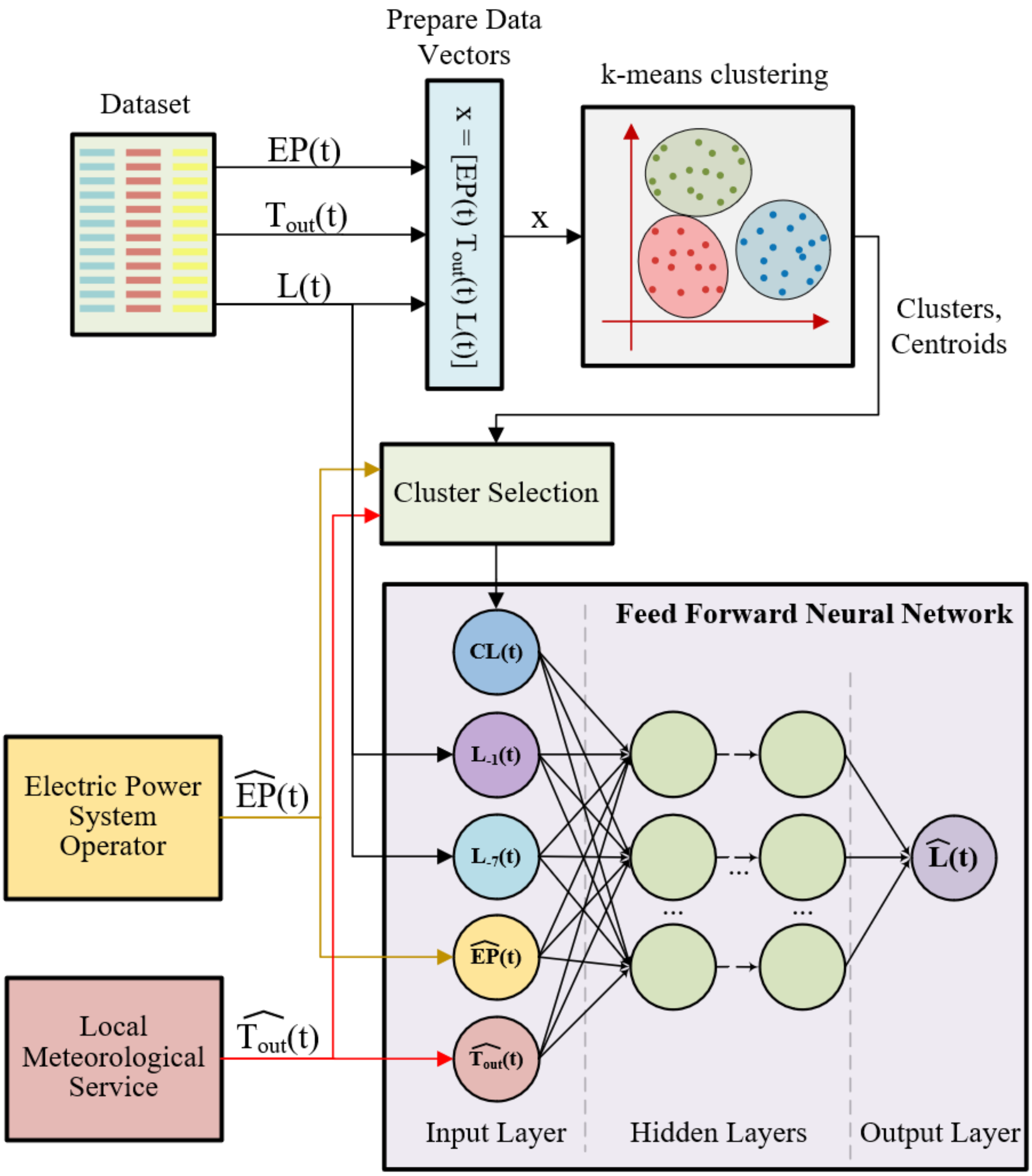

Fig. 3.2 - K-means clustering and feed-forward Neural Network for load prediction.

3.4.1 k-means Clustering

The data vector $\boldsymbol{x_i}$ that is created as the input of the clustering system and corresponds to the ith day of the examined period is defined as:

$$x_i(t) = \left[\frac{EP_i(t)}{\max\,(EP_i(t))} \quad \frac{T_{i,out}}{\max\,(T_{i,out})} \quad \frac{L_i(t)}{\max\,(L_i(t))} \right] \tag{12}$$

The x_i data vectors are fed to the k-means clustering algorithm, to obtain the optimal clusters and their centroids. The k-means clustering method partitions n observations into k clusters according to each observation's closest centroid, distance-wise. Each centroid consists of three parts, corresponding to the electricity price, temperature and load. The centroids are saved in the "Cluster Selection" block, and used in combination with the real-time forecasts of electricity price $\widehat{EP}(t)$ and outdoor temperature $\hat{T}_{out}$ to predict the residential load. The load forecast CL(t) of the clustering algorithm is used as an input to the ANN.

3.4.2 Feed-forward Artificial Neural Network

The second part of the residential load forecast system proposed in this dissertation is a feed-forward ANN. Feed-forward neural networks (FNN) are a collection of artificial nodes (called neurons) and edges with weights that adjust throughout the training process. FNNs are more computationally simple than other types of ANNs, since their edges do not form cycles. The proposed forecasting system does not require a more complex ANN, since, due to the nature of electrical loads, a base stochasticity will always exist.

As illustrated in Fig. 3.2, the input layer of the ANN comprises the forecasted electricity price and temperature, the load forecast of the k-means algorithm, last day's load demand $\mathrm{L}_{-1}(\mathrm{t})$, and the load demand of the same day of the last week $\mathrm{L}_{-7}(\mathrm{t})$. The output of the ANN, $\hat{\mathrm{L}}(\mathrm{t})$, is fed to the power optimization algorithm.

3.5 Energy Management Algorithm

In this dissertation, the power management problem of the day-ahead optimization of the residence is solved using the PSO algorithm. PSO is a metaheuristic computational method that uses a population of "particles", with each particle indicating a candidate solution. The particles are moved in the search-space of the applied problem semi-randomly, while being influenced by their own past best position and the best position the neighboring particles. Due to its metaheuristic behavior and "swarm" intelligence, PSO has been proved to be resilient for complex and non-linear optimization problems. It is able to converge on global minima in complex systems with many local minima, one category of which is power management problems.

The main objective function of this dissertation's power optimization problem is shown next:

$$\min_{\substack{P_{EV},P_B,\\ P_{EC},P_{L,sh},P_{L,sd}}} \left\{ \sum_t [(P_{EV}(t) + P_B(t) + P_{EC}(t) + P_{L,sh}(t) - P_{L,sd}(t)) \cdot \widehat{EP}(t) - P_{PV}(t) \cdot EP_{PV}(t)] \cdot dt \right\} + p_{sd} \tag{13}$$

S.t (1) - (11), (14) - (23)

The goal of the PSO algorithm is to minimize the objective function (13), therefore minimizing the daily energy cost of the residence. However, the many constraints shown before and after are also part of the main objective function, and are applied as penalties that the algorithm must try to minimize.

$$P_{EV}(t) + P_B(t) + P_{EC}(t) + P_{L,sh}(t) - P_{PV}(t) = P_G(t) \ \ \forall t \tag{14}$$

$$P_{G_{min}} < P_G(t) < P_{G_{max}} \ \forall t \tag{15}$$

$$P_G(t) = 0, \ \ t \in [t_{os}, t_{oe}] \tag{16}$$

$$P_{EV}(t) + P_B(t) + P_{EC}(t) + P_{L,sh}(t) = P_{L,sd}(t) + P_{PV}(t), \qquad t \in [t_{os}, t_{oe}] \tag{17}$$

$$p_{sd} = \sum_{t=t_{os}:\delta t:t_{oe}} a \cdot P_{L,sd}(t) \cdot dt \tag{18}$$

$$0 \leq \ P_{L,sd}(t) \leq P_{L,sh}(t) \tag{19}$$

$$P_{L,sd}(t) = 0, \qquad t \notin [t_{os}, t_{oe}] \tag{20}$$

where P_{EV} and P_B are the powers of the EV and the home battery respectively, P_{EC} is the power consumption of the HVAC, $P_{L,sh}$ is the electrical load demand after the load shifting application, P_{PV} is the power production of the PV panels, P_G is the power exchanged by the MPC and the power grid, EP_{PV} is the price the PV energy is sold and $\widehat{EP}$ is the forecasted electricity price. The constant a is set by the microgrid operator to manage the weight of load shedding in the objective function.

In constraint (14), the power balance and power flows of the prosumer residence and each of its power components can be seen. The technical minimum and maximum power transfer values at the PCC are defined in (15). The autonomous operation constraints for power balance are featured in (16) and (17), starting at t_{os} and ending at t_{oe}. If the residence is unable to meet local demand during autonomous mode, loads can be shed by an amount of power $P_{L,sd}(t)$ as seen in (17), (19) and (20). To reduce load shedding as much as possible, a corresponding penalty (18), p_{sd}, is added to the objective cost equation.

3.5.1 Demand Response

The prosumer residence has the capability of load management through a DR system. The DR system affects the flexible loads of the residence, and ignores the HVAC system and the critical loads. It is assumed that part of the active loads forecasted by the aforementioned load forecast system can be shifted or shed as defined in (21) and (22). Energy balance before and after load shifting at the end of the day is ensured by (23).

$$P_{L,sh}(t) = \big(1 + LS(t)\big) \cdot P_L(t)\ \forall t \tag{21}$$

$$LS_{min} \leq LS(t) \leq LS_{max}\ \ \forall t \tag{22}$$

$$\sum_t \big(P_{L,sh}(t)\big) = \sum_t \big(P_L(t)\big) \tag{23}$$

where $P_{L,sh}$ and P_L is the shifted and the original load power consumption respectively, and LS is the load shifting factor. The differentiation between critical and flexible loads is done with an arbitrary percentage of the total power consumption being from flexible loads, as defined by the microgrid operator in LS_{min} and LS_{max}.

3.6 Frequency Support Mechanism

As mentioned before and illustrated in Fig. 3.1, the HEMS is equipped with real-time detection of frequency deviations in order to provide frequency support to the grid if it is required. More specifically, the PLL is fed with the grid-side voltage measurement to estimate voltage phase angle θ and then system frequency through the differentiation of θ.

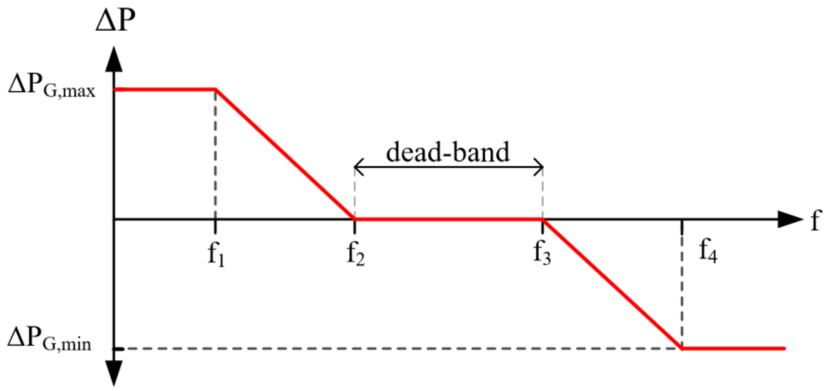

Fig. 3.3 – Droop frequency characteristic.

If the frequency deviations measure outside of the predefined dead-band seen in Fig. 3.3, the proposed HEMS can provide support through suitable regulation of the active power exchange at the grid coupling point. The dead-band range is set at f_2 = 49.8 Hz, f_3 = 50.2 Hz, the floor and ceiling of the droop characteristic at f_1 = 49.2 Hz and f_4 = 50.8 Hz. The required change of power between the grid and MPC is determined using the frequency droop control method according to (24) and Fig. 3.3,

$$\Delta P_G(f) = \begin{cases} \Delta P_{G,min} & f < f_1 \\ \Delta P_{G,min} - \dfrac{\Delta P_{G,min}}{f_2 - f_1}(f - f_1) & f_1 \le f \le f_2 \\ 0 & f_2 \le f \le f_3 \\ \dfrac{\Delta P_{G,max}}{f_4 - f_3}(f - f_3) & f_3 \le f \le f_4 \\ \Delta P_{G,max} & f > f_4 \end{cases} \tag{24}$$

where ΔP_G is the deviation from the setpoint of the active power as set by the energy management algorithm, and $\Delta P_{G,max}$ and $\Delta P_{G,min}$ are the maximum and minimum values of ΔP_G respectively. These two values are derived from all the previous constraints of the HEMS and can change real-time, depending on each power component and the maximum power transfer capabilities of the PCC.

3.6.1 Optimal flexibility

The calculated power deviation ΔP_G has then to be split optimally amongst the three power components of EV battery, home battery and residential flexible loads. This optimal split ensures the power change is achieved, but also that each component maintains the highest possible flexibility. The optimization problem is solved real-time, using MATLAB's constrained nonlinear function *fmincon*. The goal of the function is to reduce component flexibility as little as possible, while also achieving the power change calculated by the droop characteristic.

$$\max_{P_{EV},P_B,P_L} \begin{pmatrix} w_{EV} \cdot flex_{EV}(t) \\ +w_B \cdot flex_B(t) + w_L \cdot flex_L \end{pmatrix} \tag{25}$$

S.t (1) - (11), (14) - (23), (27) - (29).

$$\max_{P_{EV},P_B,P_L} \begin{pmatrix} w_{EV} \cdot flex_{EV}(t) \\ +w_B \cdot flex_B(t) + w_L \cdot flex_L \end{pmatrix} \tag{26}$$

$$\Delta P_G(t) = \Delta P_{EV}(t) + \Delta P_B(t) + \Delta P_L(t) \quad \forall t \tag{27}$$

$$flex_s(t) = \begin{cases} \dfrac{E_{s,max} - E_s(t+dt)}{E_{s,max} - E_{s,min}}, & \Delta P_{\mathrm{G}} > 0 \\ \dfrac{E_s(t+dt) - E_{s,min}}{E_{s,max} - E_{s,min}}, & \Delta P_G < 0 \end{cases}, \qquad s \in [EV, B, L] \tag{28}$$

$$w_s = 0.5 \cdot \left(\frac{E_s, max}{E_{EV,max} + E_{B,max} + E_{L,max}} + \frac{P_{s,max}}{P_{EV,max} + P_{B,max} + P_{L,max}} \right) \tag{29}$$

$$E_s(t+dt) = E_s(t) + P_s(t) \cdot dt \quad s \in [EV, B, L] \tag{30}$$

$$E_L(t) = \sum_{t=0:dt:t} P_L(t) \cdot dt \ , \quad E_{L,max}(t) = \sum_{t=0:dt:T} P_L(t) \cdot dt \tag{31}$$

where $flex_s$ and w_s are the flexibilities and the weights for the EV battery, home battery and residential loads.

The flexibility of each power component is defined by its capability to alter its output with regard to the resulting movement towards its operational limits. For the two ESSs, this means that the flexibility is linked to the distance between the resulting energy level and its predetermined bounds. The estimation of the flexibility depends on the sign of the change of the power the MPC exchanges with the grid. Due to load convention, positive ΔP_G associates flexibility with the upper limit of $E(t)$, and negative ΔP_G with the lower limit of $E(t)$.

The flexibility of the residential electrical loads, as defined in (28), is proportional to the normalized distance from their maximum or minimum energy values according to the sign of ΔP_{G}. The energy of loads $E_L(t)$ is defined as the energy consumption of the residential loads throughout the day, and $E_{L,\max(min)}$ is the maximum (minimum) possible change in their energy consumption through load shifting, as shown in (30) and (31). The weight of each power component's flexibility is defined in (29) as the normalized sum of their max energy levels and powers.

4.
Results

After having analyzed all the mechanisms and algorithms that make up the HEMS, this chapter will be about the simulation results of several different scenarios. The residential load forecasting system, the day-ahead power optimization, the optimal frequency support system and the economic efficiency of the whole HEMS are evaluated.

4.1 General modelling

In this subchapter, simulation parameters that apply to all examined scenarios are analyzed.

The presented scenarios are simulated on a summer day with high environment temperature and ample sunlight with little cloud cover. Using solar irradiation forecasts, the HEMS estimates the power production of the PV arrays as seen in Fig. 4.1. As expected, peak solar power production is around noon.

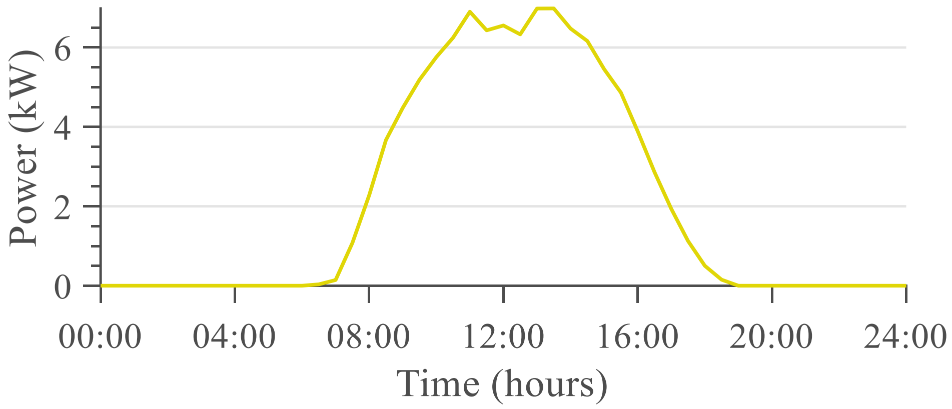

Fig. 4.1 - PV array power production.

The day-ahead optimization is executed on a 24-hour basis, from midnight to midnight, with the examined 24-hour period divided into 15-min intervals. The model parameters of the emulated residential prosumer are listed in Table 1.

Table 1 - Model Parameters

	Parameters	Values	Units
Electric Vehicle	$P_{EV,max}$	5	kW
	$P_{EV,min}$	-5	kW
	$E_{EV,Rated}$	35	kWh
Home Battery Pack	$P_{B,max}$	3	kW
	$P_{B,min}$	-3	kW
	$E_{B,Rated}$	15	kWh
PV arrays	$P_{PV,Rated}$	7	kW
Multi-Port Converter	$P_{G,max}$	10	kW
	$P_{G,min}$	-10	kW
Thermodynamic Model	ρ	1.2	kg/m^3
	C	1/3600	$kJ/(kg \cdot °C)$
	V	729	m^3
	U_{wall}	0.00048	$kW/(m^2 \cdot °C)$
	F_{wall}	405	m^2
	U_{win}	0.0029	$kW/(m^2 \cdot °C)$
	F_{win}	150	m^2
	α_w	18.63	-
	R_{sej}	0.04	$m^2 \cdot °C/W$
	t_{win}	1.1	-
	SC	0.54	-
Heating/Cooling System	$P_{EC,max}$	3	kW
	$P_{EC,min}$	0	kW
	$T_{in,max}$	23	$°C$
	$T_{in,min}$	20	$°C$
	COP	3.5	-

The EV battery is simulated after the battery of the Nissan Leaf, an affordable EV with modest energy capacity. The home battery pack is simulated after Tesla's Powerwall, a rechargeable lithium-ion battery system designed for residential installations. For the purpose of the thermodynamic model, the residence is modelled as a two-story building with an area of 81 square-meters per floor. The height of each floor is 4.5 meters.

4.2 Load forecast results

The temperature time-series used as input to train the k-means clustering algorithm and the ANN were downloaded from VisualCrossing. The temperature dataset features the months of June, July and August for the city of Chania, and the total range of temperature can be seen in Fig. 4.2, as well as the mean temperature of the three summer months. Additionally, the blue plotted line is the selected daily temperature used in the following examined scenarios as the environment temperature.

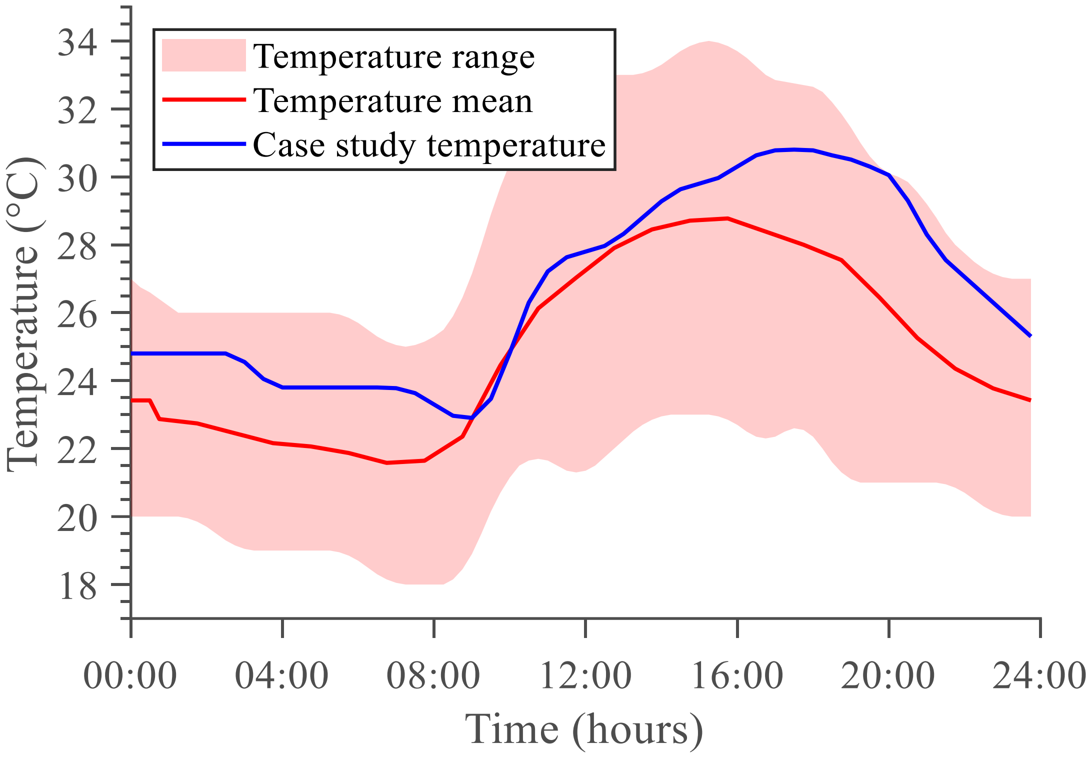

Fig. 4.2 - Environment temperature dataset used for training.

Similarly, the cost of energy time-series used for the training of the load forecast system were downloaded from ΑΔΜΗΕ for the months of June, July and August for Greece, as seen in Fig. 4.3. The red plotted line is the mean of the energy price for the three months, and the blue line is the randomly selected daily time series used for the simulated scenarios in the following subchapters. Additionally, Fig. 4.4 shows the simulated loads used for training the load forecasting system.

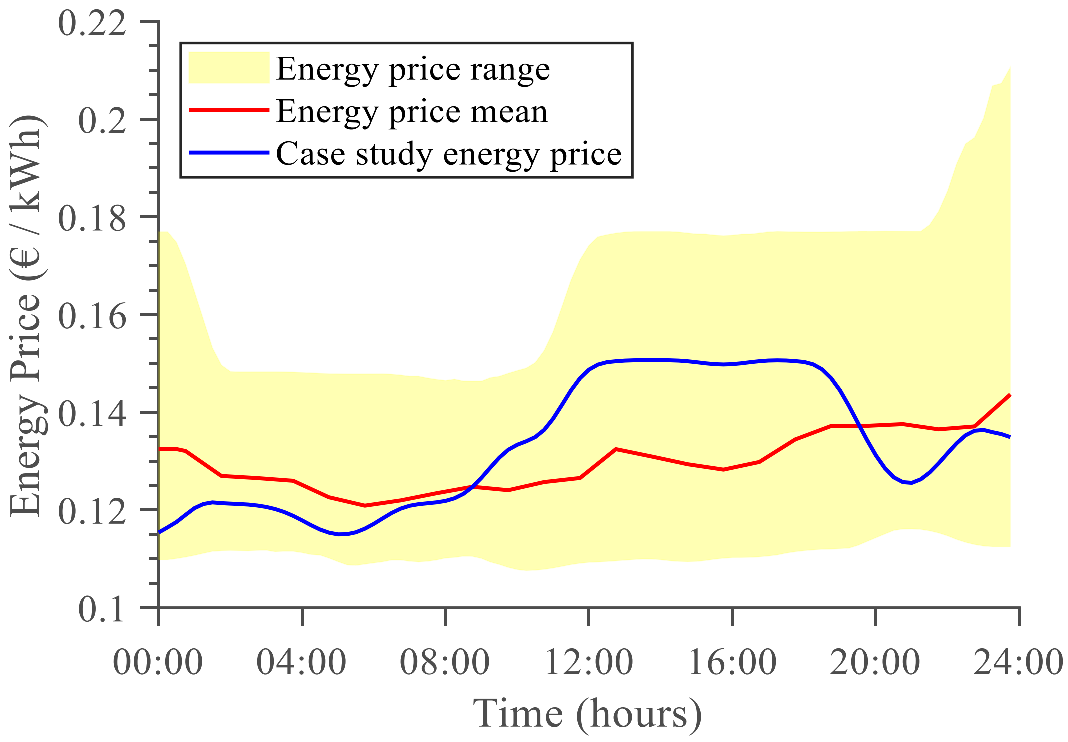

Fig. 4.3 - Electricity price dataset used for training.

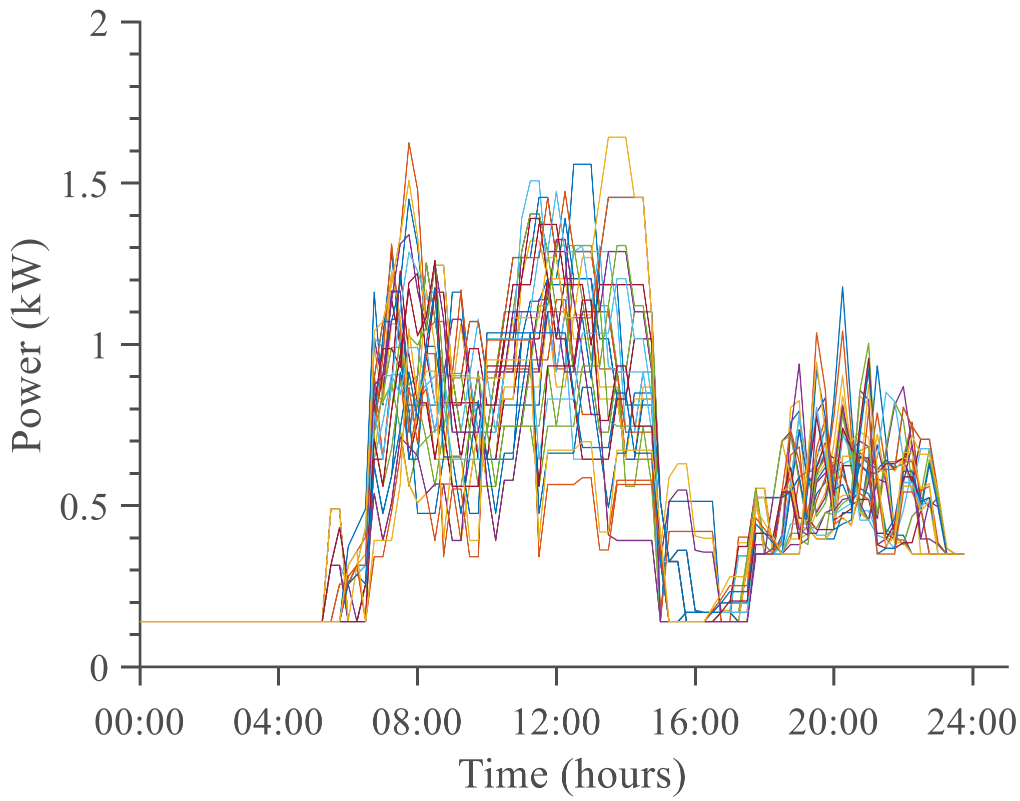

Fig. 4.4 - Simulated loads used for training.

Once the forecasted energy cost, environment temperature and simulated loads are complete, 80% of the samples are fed to the load forecasting system and used for training. The rest 20% of samples will be used later for validation.

By the time the k-means clustering algorithm and the ANN have concluded their training, their effectiveness can be evaluated using the samples of the dataset left for testing. In Fig. 4.5, the error histogram of the ANN is illustrated. Error histograms are the histograms of the errors between target values and predicted values after training the feedforward neural network. It can be seen that the number of instances with an error of 8-15% is substantial. Considering, however, the high stochasticity of residential loads that makes their forecasting a challenging procedure, the ANN's performance is deemed adequate.

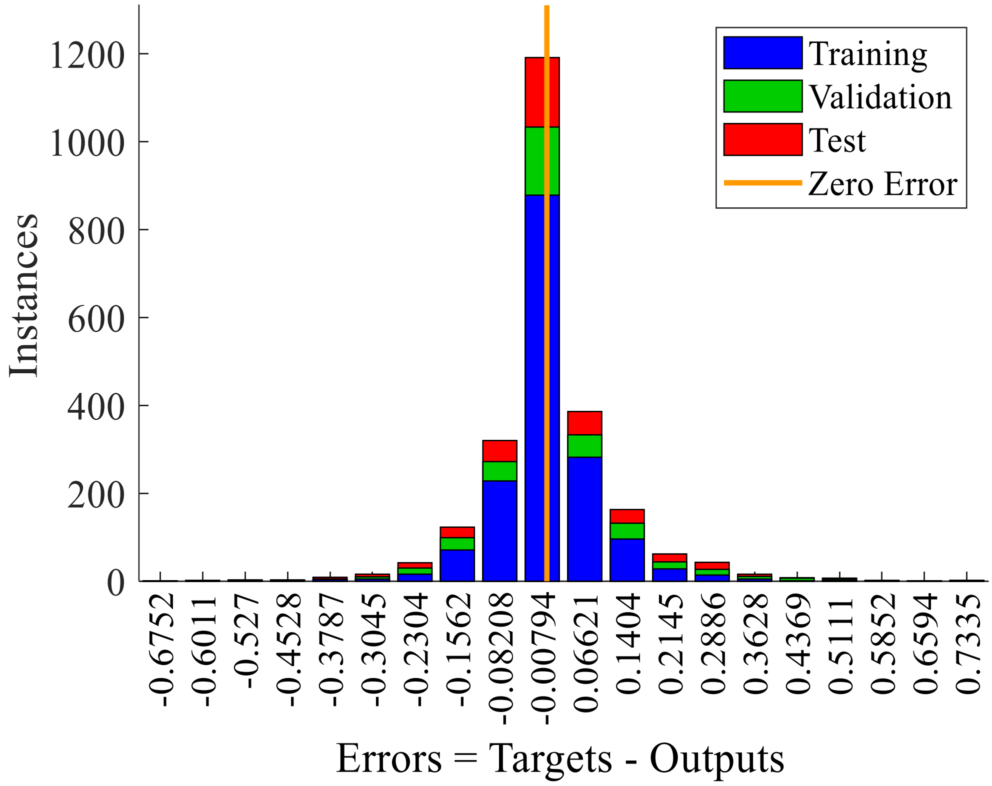

Fig. 4.5 - Error histogram of the evaluation of the ANN.

In the following Fig. 4.6, a comparison between the testing samples of the dataset and the predictions of the load forecast system for those testing samples are shown. It can be seen that, while not perfect, the predictions are close to the real values.

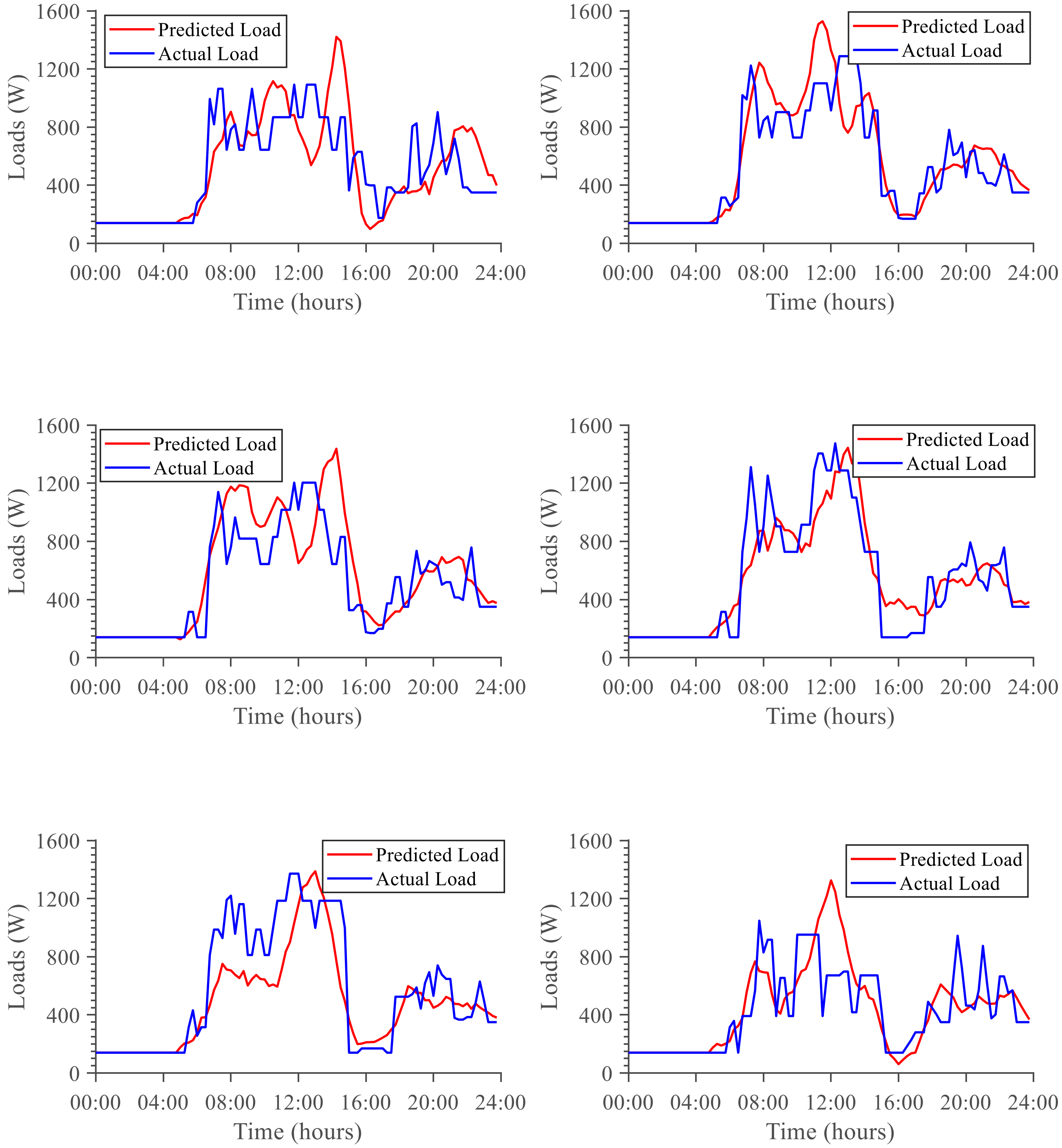

Fig. 4.6 - Load forecast test data comparison with system predictions.

4.3 Day-ahead optimization results

In this chapter, the results of the general day-ahead optimization by the HEMS for the prosumer residence are analyzed. Four different scenarios are simulated in order to get a clearer view of all the capabilities and economic efficiency of the proposed HEMS. Scenario A features an optimal, fault-free day with 24h presence of the EV, scenario B features a period during which the residential microgrid disconnects from the grid, scenario C features a frequency deviation and an EV commute, and finally scenario D is the “dumb” mode, during which there is no smart utilization of any power component.

4.3.1 Operation Scenario A – Optimal day

As shown before in Fig. 4.3 (blue plotted line), the electricity price reaches its peak in the noon-afternoon hours and dips during the early morning and night hours. As the HEMS is tasked with increasing economic efficiency, it actively schedules the batteries to absorb active power during low electricity price periods in order to minimize charging costs. Subsequently, energy is discharged from the batteries to be sold to the grid during peak demand, when electricity price is at its highest. This trend can be noticed in Fig. 4.7, where both batteries are scheduled to charge during early morning and late-night hours, and are scheduled to discharge and sell their energy during noon and afternoon.

Additionally, constraint (4) is used to set the end-of-the-day energy level of both batteries to be the same as the initial energy level at the start of the day-ahead optimization. This is done to achieve comparison fairness between different executions of the algorithm.

At the bottom two plots of Fig. 4.7, the scheduling of the HVAC system can be seen. The thermodynamic model analyzed above is used to predict the residence temperature and plan the power consumption of the HVAC accordingly, in order to maintain indoor temperature in the predetermined comfortable levels.

The demand response mechanism of the HEMS is illustrated in Fig. 4.8. The algorithm schedules the flexible loads away from the high electricity price periods to those ones of low electricity price.

To summarize the power management of the residence, the power exchange between the prosumer residence and the grid is depicted in Fig. 4.9. The power exchange follows the opposite trend of the electricity price, similarly to how the batteries are scheduled to charge and discharge. Energy is sold to the grid when electricity price is high (green area) and bought from the grid when price is low (red area). The large amount of power sold during noon hours is attributed to the increased PV power generation of that time period.

For this scenario, the daily energy cost is predicted to be -2.39€, i.e., the microgrid user made a profit of 2.39€.

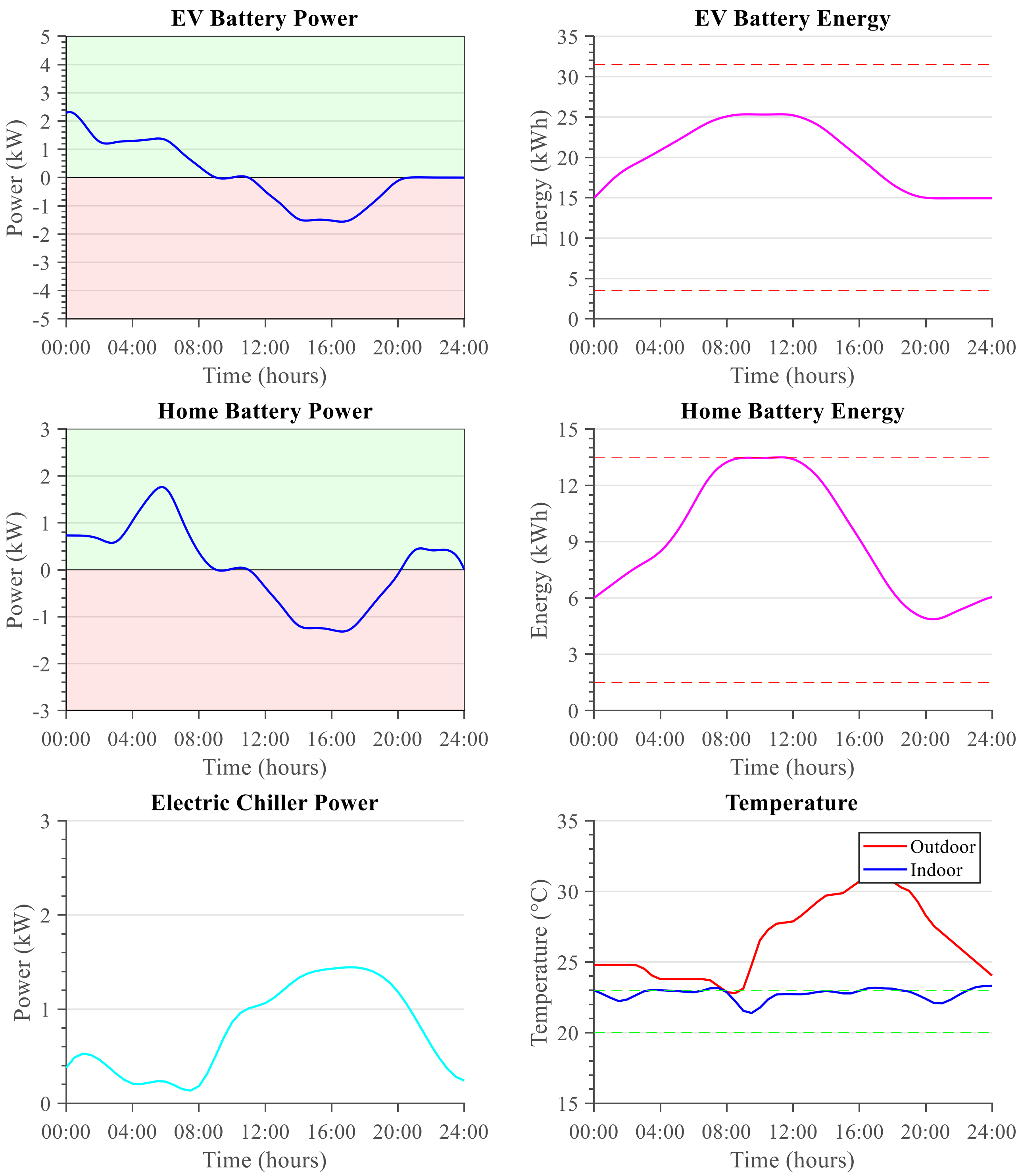

Fig. 4.7 – Optimization of EV, home battery and HVAC power components – Scenario A.

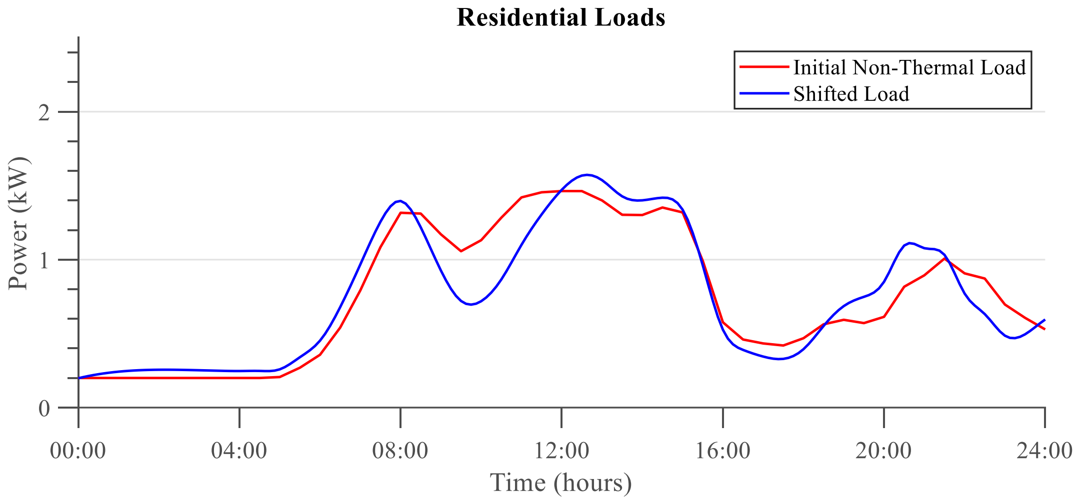

Fig. 4.8 - Load shifting of non-thermal home loads – Scenario A.

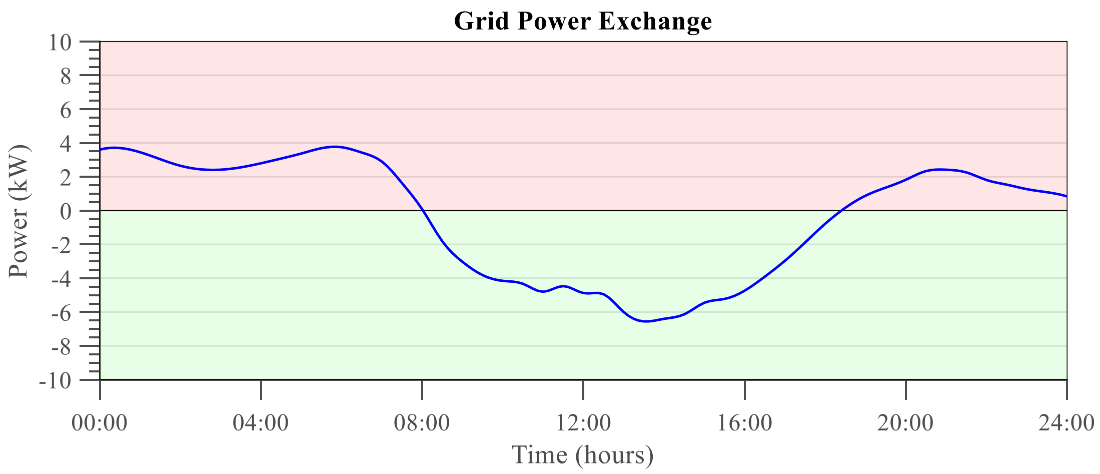

Fig. 4.9 – Power exchange between prosumer residence and power grid – Scenario A.

4.3.2 Operation Scenario B – Microgrid islanding

In the second scenario, a disconnection from the grid is simulated, where the HEMS must operate independently for a few hours. As can be seen in Fig. 4.10 and Fig. 4.12 as a gray area, the prosumer disconnects from the grid from 15:30 until 19:00. This disconnection from the grid is already planned beforehand, and not a real time event. It is therefore part of the day-ahead optimization process.

The prosumer disconnects from the grid at 15:30, but the PV arrays can still produce enough energy to cover the loads for the next 2 hours (Fig. 4.1). The excess PV energy is therefore stored in the two batteries. By 17:00, PV generation has dropped significantly, and the stored ESS energy must be used to supply the residential loads until the end of the islanded operation.

The autonomous period is seen clearly in Fig. 4.12, as the time period with no power exchange with the grid. For that period, the HEMS must maintain power balance through its power components, as shown in constraint (17).

For this scenario, the daily energy cost is predicted to be -2.26€.

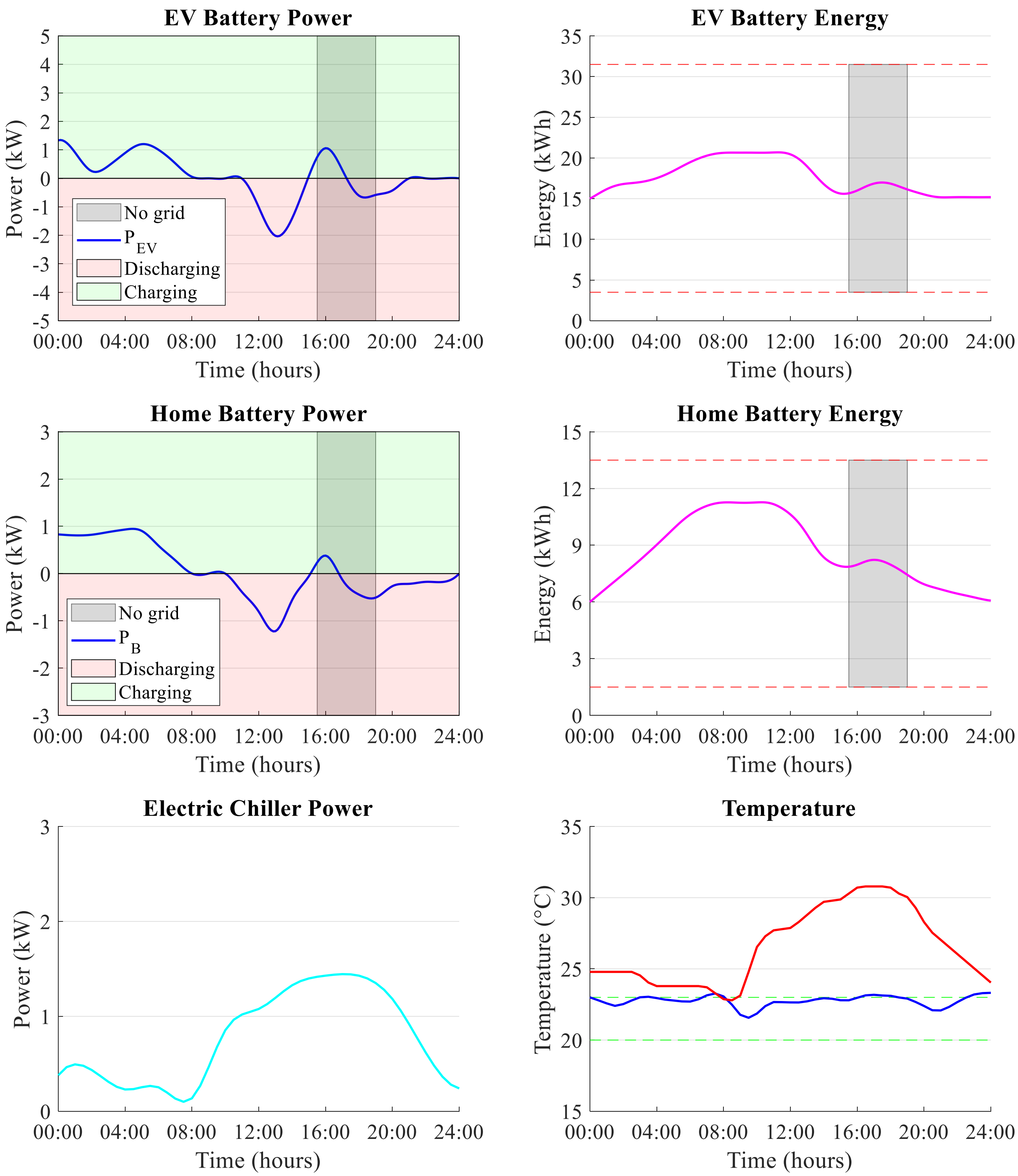

Fig. 4.10 – Optimization of EV, home battery and HVAC power components – Scenario B.

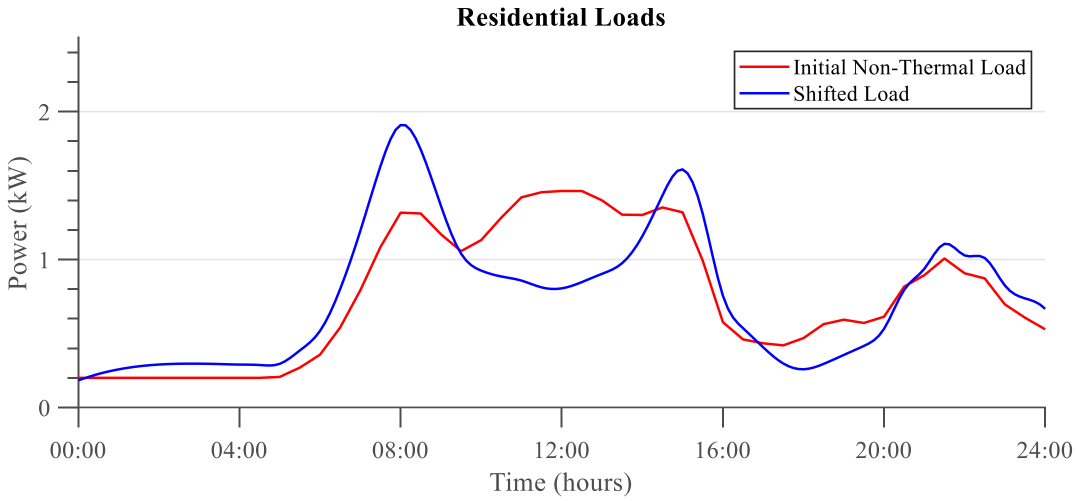

Fig. 4.11 - Load shifting of non-thermal home loads – Scenario B.

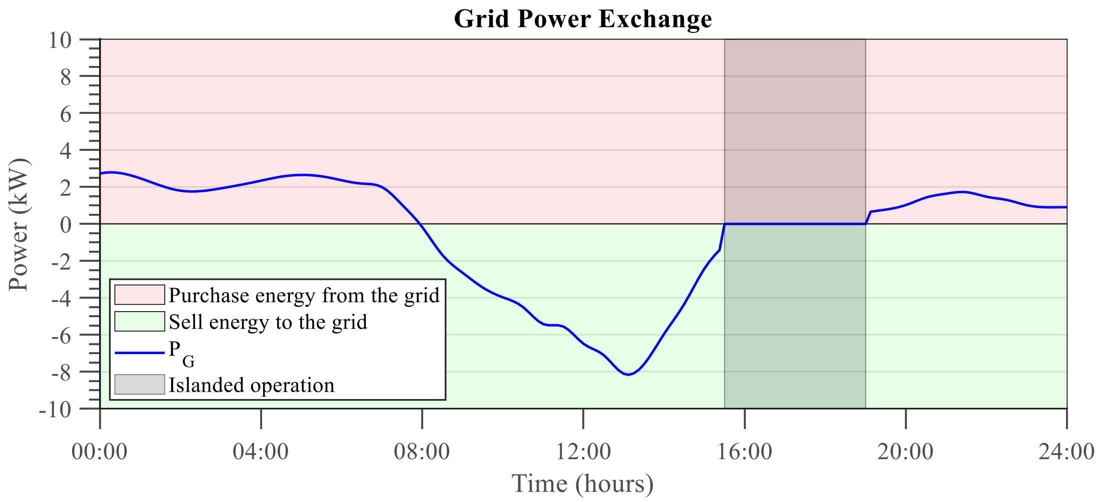

Fig. 4.12 – Power exchange between prosumer residence and power grid – Scenario B.

4.3.3 Operation Scenario C – Frequency Support

The third simulated scenario features a 10-minute frequency deviation in the grid's frequency, as shown in Fig. 4.13. The frequency initially dips to 48.9Hz, but is restored to 49.6Hz after primary frequency response activates. The slower secondary frequency control of the power system then stabilizes the frequency over the next 10 minutes to 50Hz.

By applying the droop characteristic method explained in Fig. 3.3 and equation (24), we can calculate the required power change that the HEMS needs to achieve in order to support the grid. This power change can be seen in Fig. 4.14 as the plotted red line. Most of the power change required to support the grid in total wattage is during the first 30 seconds of the frequency deviation.

The power adjustments made to the EV, home battery and residential load during the frequency drop are also shown in Fig. 4.14. The residential load is first shifted to its max limit. Once it is unable to ensure ΔP_G, the EV battery and the home battery provide extra power to the grid. Since, as seen in Fig. 4.16, the EV battery is more charged than the home battery at the time of the frequency drop (11:10), the EV battery has higher flexibility and therefore has more power drawn from it.

When the value of the grid's frequency falls into the dead zone following the under-frequency event, the components of the residential microgrid revert to the power set-points established by the HEMS during the original day-ahead power optimization. The day-ahead optimization however is rerun for the rest of the day until midnight, in order to account for any deviations present in the system due to the power change required by the ancillary services.

An EV commute is also simulated in this scenario, shown as the gray box in the EV power and energy levels of Fig. 4.16.. The EV is scheduled by the microgrid user to be absent during the hours of 16:30 until 19:30. The HEMS ensures that the battery of the EV is charged sufficiently for the desired commute. The required energy level before the commute can also be controlled by the microgrid user.

For this scenario, the daily energy cost is predicted to be -2.21€, assuming there are no financial incentives by the power aggregators for providing frequency support to the grid.

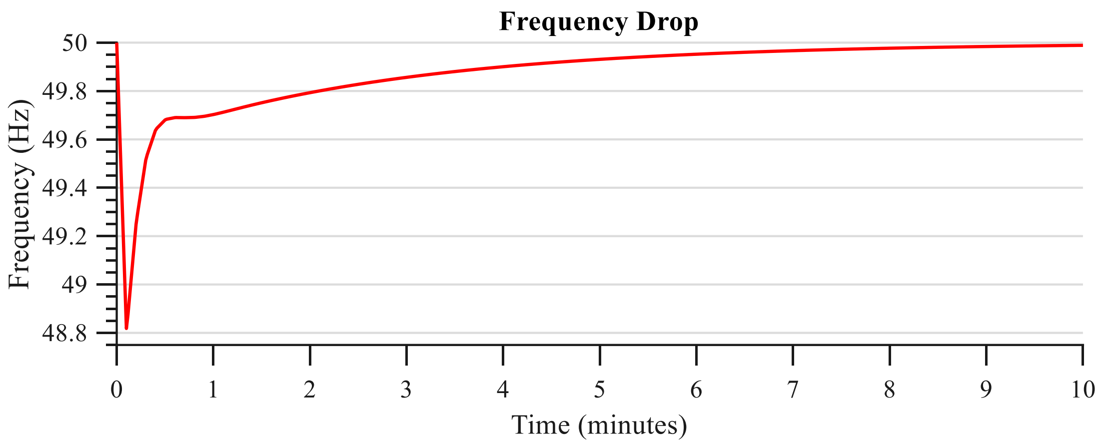

Fig. 4.13 - Grid frequency drop.

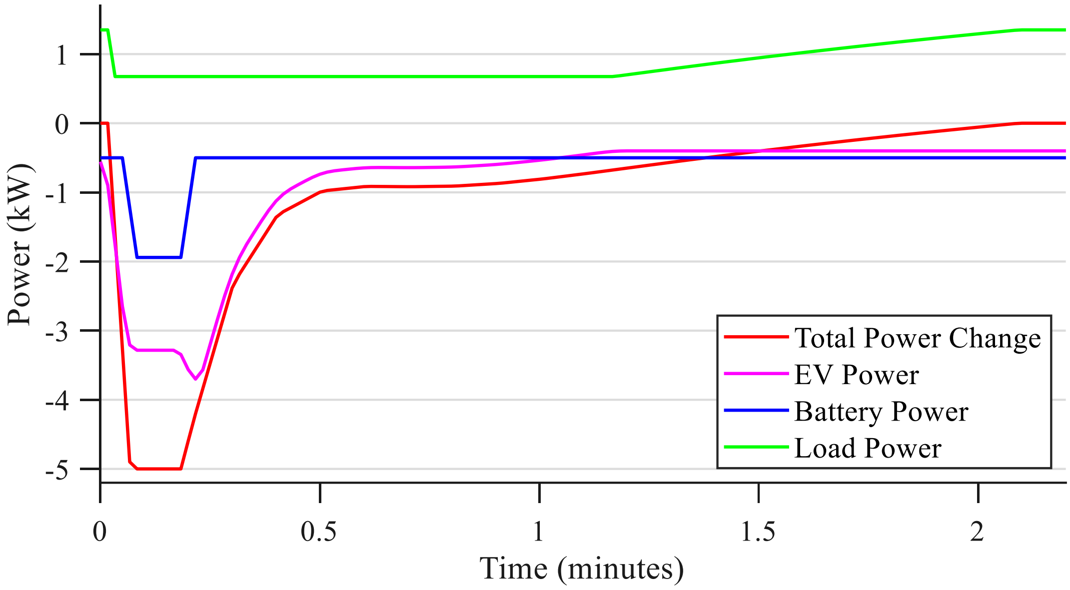

Fig. 4.14 - Total required power change, and power change of EV battery, Home Battery and Residential loads during under-frequency.

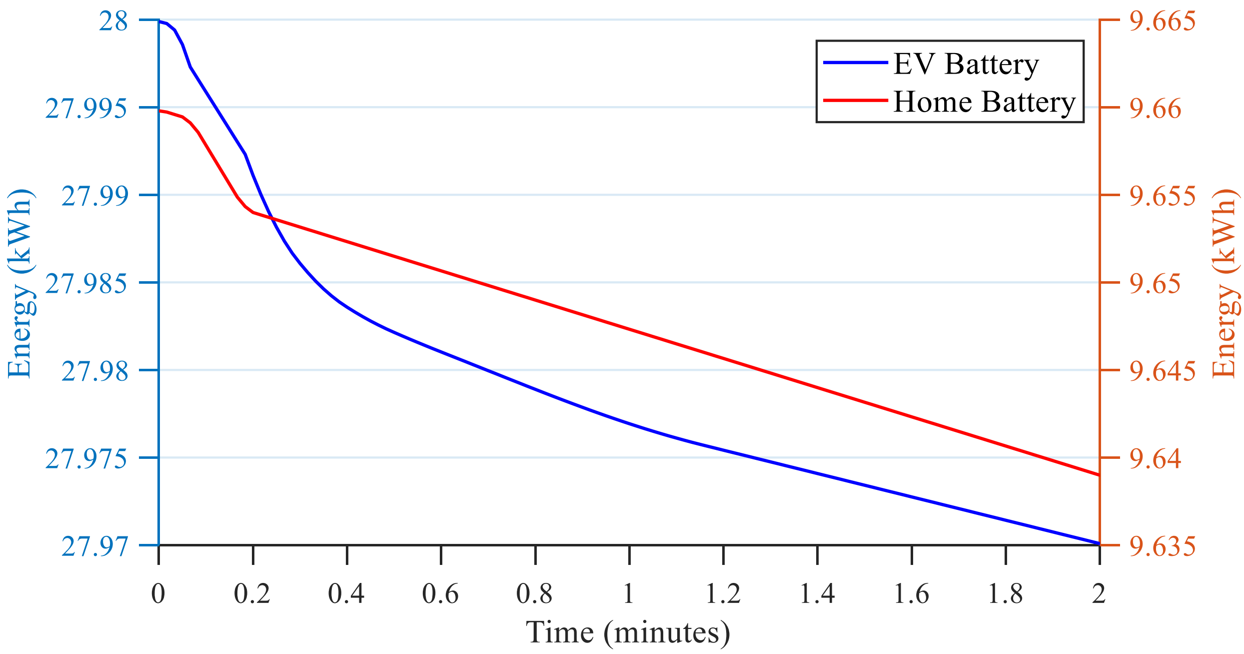

Fig. 4.15 - Energy stored in EV and home batteries during frequency drop.

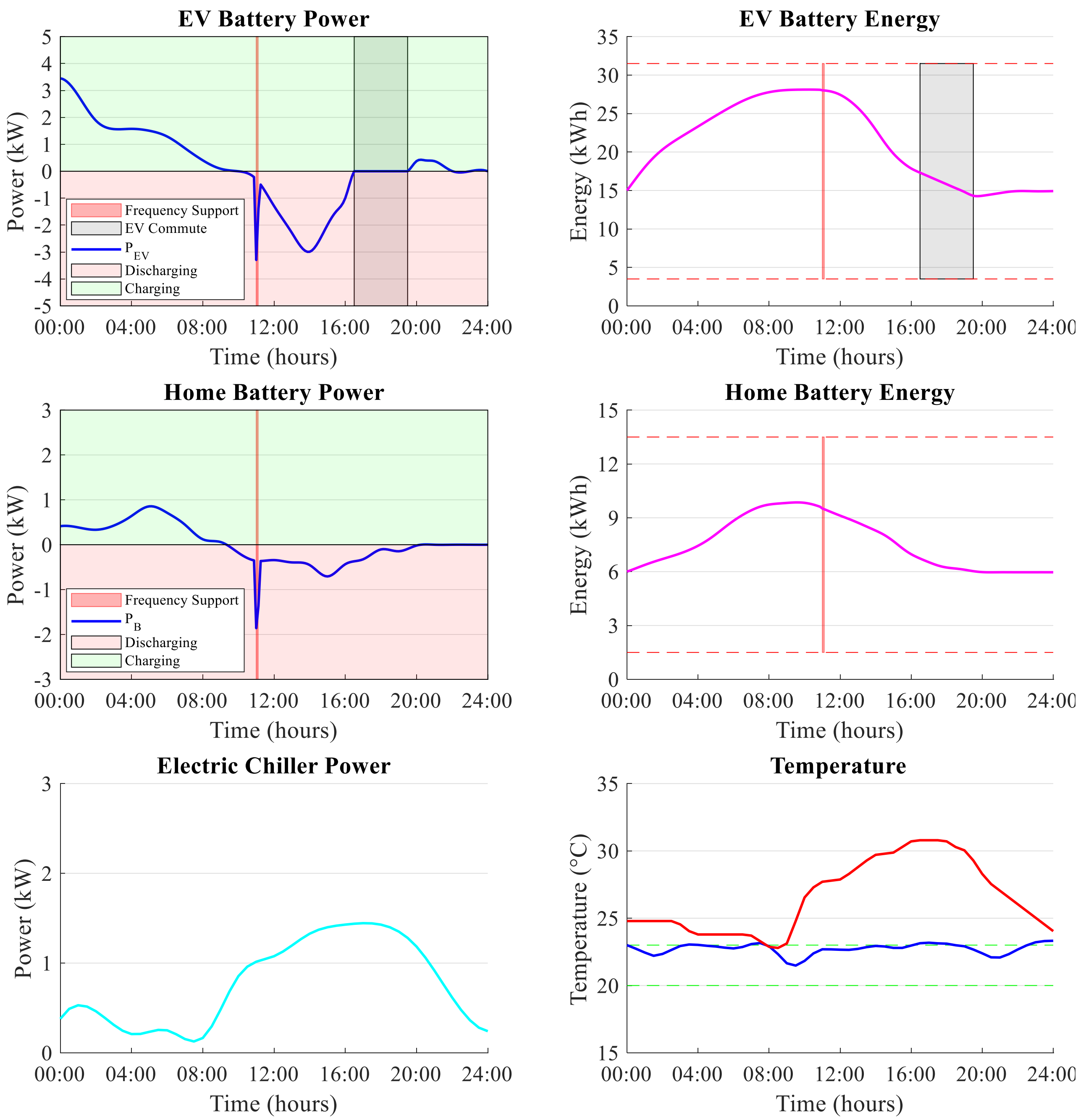

Fig. 4.16 - Optimization of EV, home battery and HVAC power components – Scenario C.

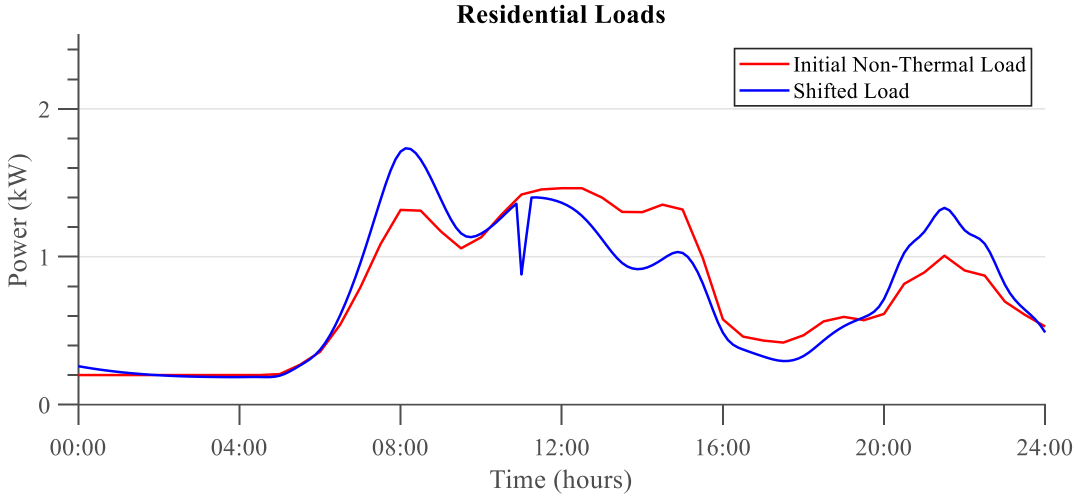

Fig. 4.17- Load shifting of non-thermal home loads – Scenario C.

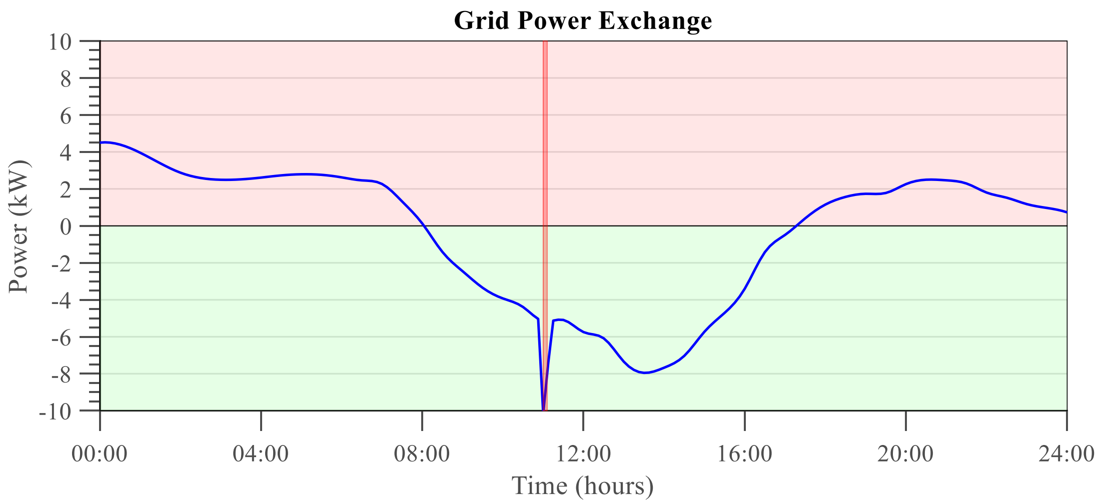

Fig. 4.18 - Power exchange between prosumer residence and power grid – Scenario C.

4.3.4 Operation Scenario D – Dumb residence

The last scenario's main feature is the lack of any smart management of any power component. The two batteries are not interacted with, there is no demand response, and the HVAC system consumes power only to maintain comfortable temperature. This scenario is simulated purely to provide a baseline as a comparison for the economic efficiency of the HEMS and its algorithms.

The daily energy cost is predicted to be -2.12€.

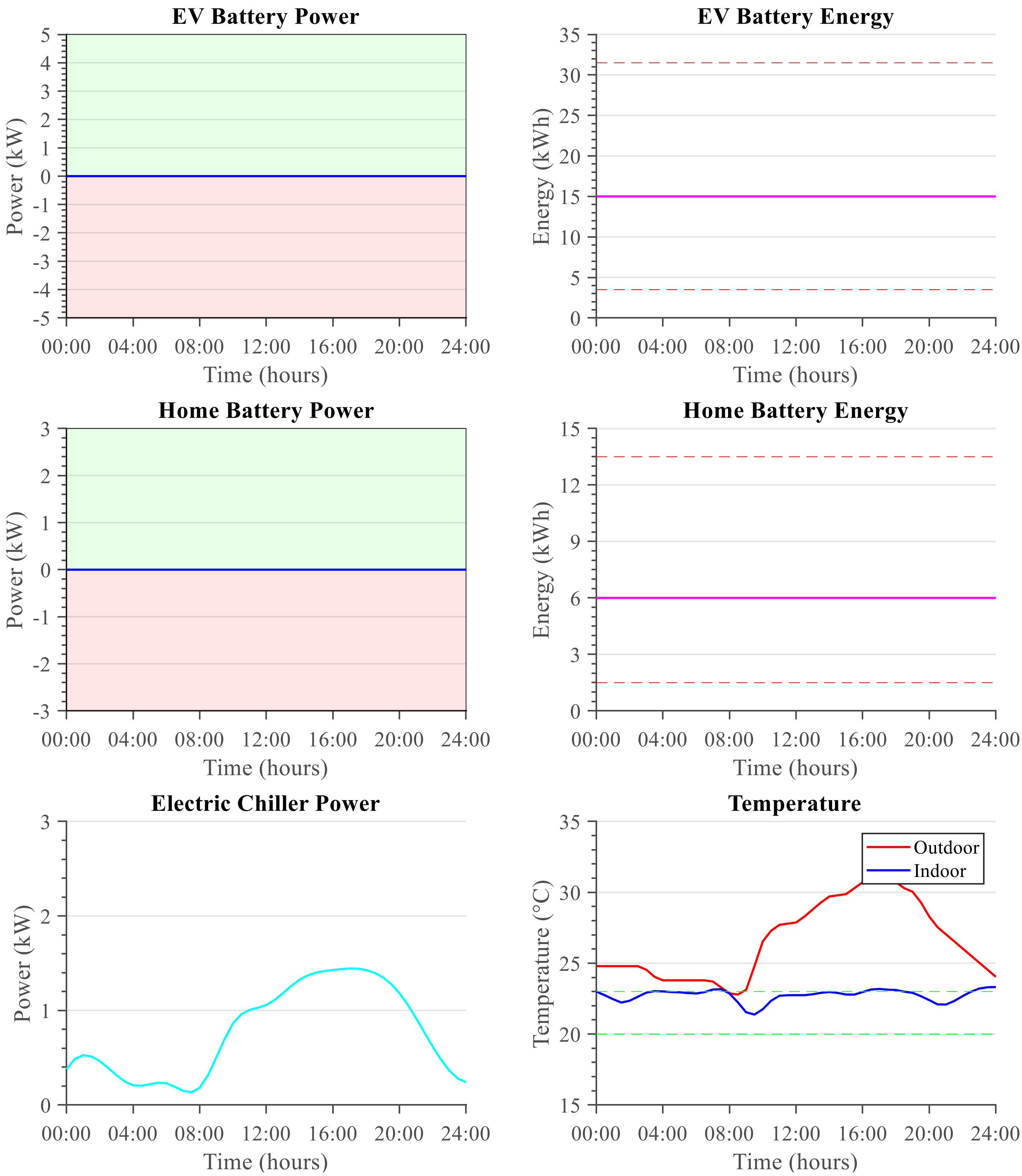

Fig. 4.19 - Optimization of EV, home battery and HVAC power components – Scenario D.

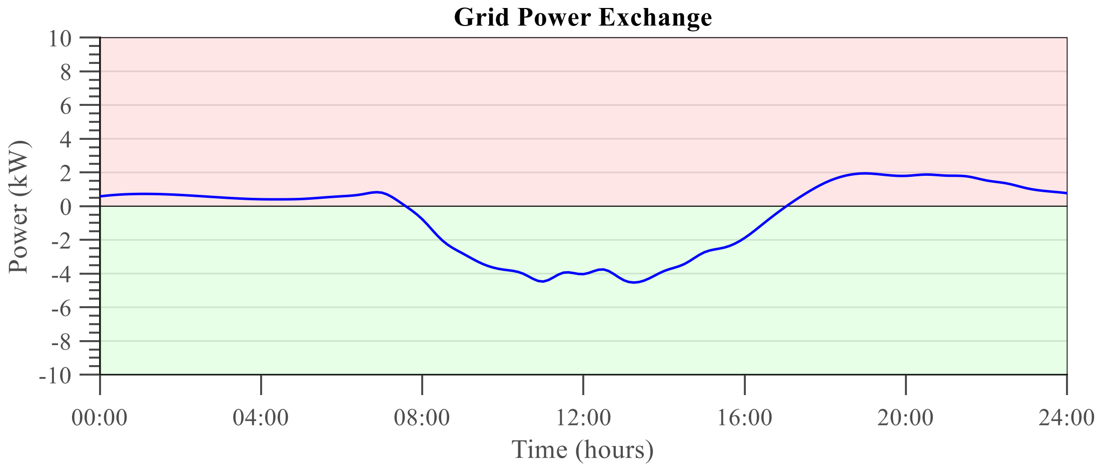

(b)

Fig. 4.20 - Power exchange between prosumer residence and power grid – Scenario D.

4.4 Cost analysis

The economic analysis of the HEMS regarding its cost saving through power management is performed by comparing Operation Scenarios A and D. Scenario A is the optimal scenario that features no islanding, frequency deviations or EV absence, and scenario D is the "dumb" scenario during which no power optimization is performed on the power components, and the electric and thermal loads are satisfied only by the PV and the grid.

The first step is to remove PV production profits from the equation, since it is a constant for both scenarios and would skew the resulting percentages. By disregarding PV production, the daily electricity cost amounts to 0.94€ and 1.21€ for scenarios A and D, respectively. Thus, in the case study under consideration, the suggested HEMS delivers a 25% cost decrease.

Multiple different final cost results of the day-ahead optimization algorithm are shown in Fig. 4.21 and Fig. 4.22. The results were obtained by changing the temperature, solar irradiance and energy cost inputs of the algorithm according to existing summer days in the database. The histogram of Fig. 4.21 highlights the varying cost saving between each different day. The overall performance of the algorithm can be observed in Fig. 4.22, with the cost saving of 40 different experiments/days visible in the plot. The blue line represents the threshold where the HEMS operates as efficiently as the dumb operation. The green area above the blue line is characterized by the HEMS performing better than the dumb operation, reducing the total daily cost. Average cost difference is valued at 24%, i.e., the algorithm averages 24% cost saving for this specific prosumer residence. However, with batteries of larger capacity, faster charging ports and more flexible loads, the cost can be decreased even further than 24%.

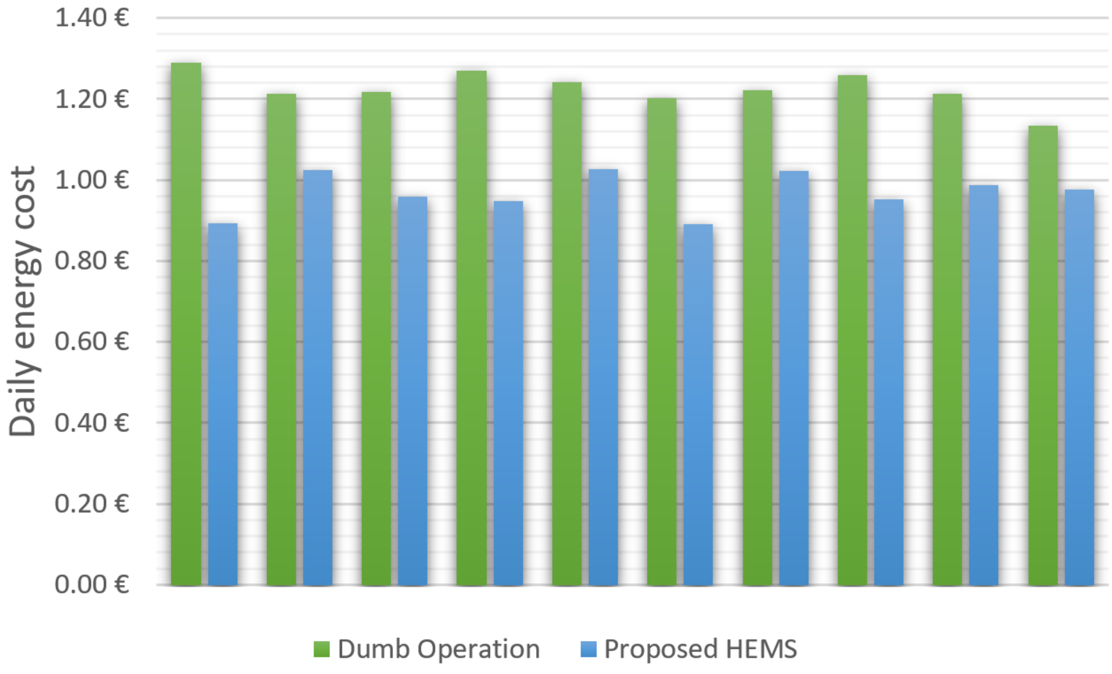

Fig. 4.21 – HEMS vs Dumb operation cost comparison histogram

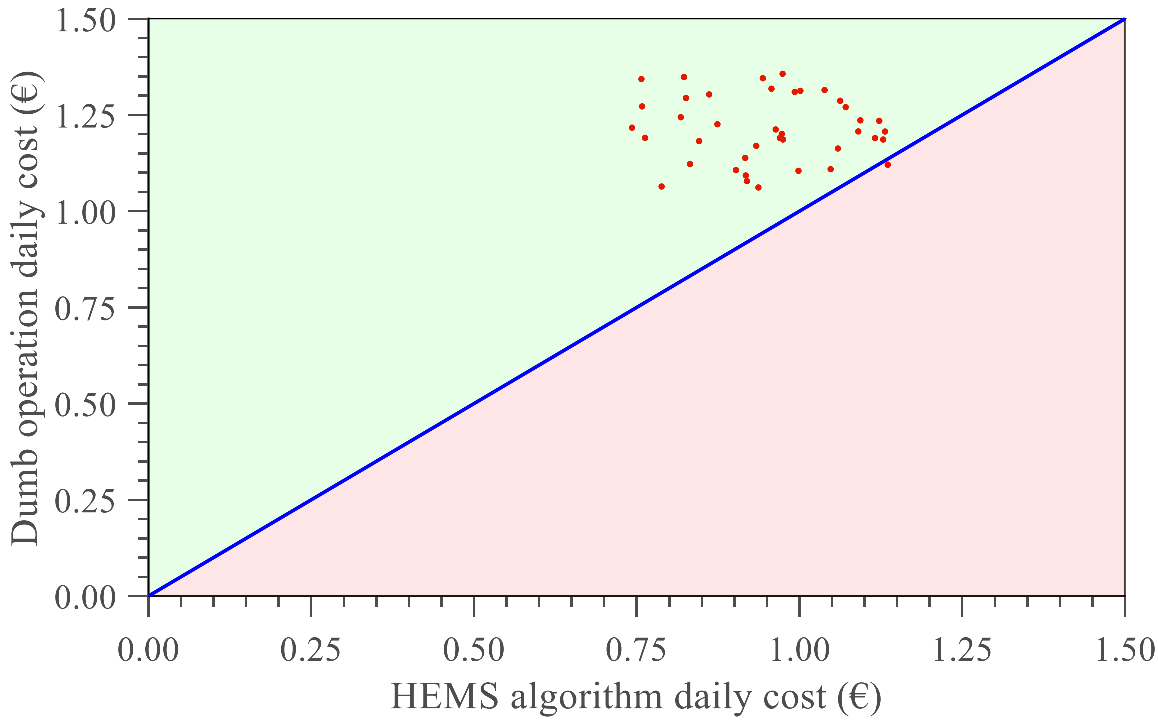

Fig. 4.22 - HEMS vs Dumb operation cost comparison plot

4.5 Experimental setup of the HEMS

The HEMS was tested on an experimental low-voltage prototype. The prototype includes the four power sources, the MPC, the grid connection and the HEMS control system, as seen in Fig. 4.23. The PC runs the HEMS software, which controls the microcontrollers that are responsible for the communication, proper operation and feedback of the circuit.

The HEMS interfaces with the user through a Graphical User Interface (GUI), visible on the PC screen to the left of Fig. 4.23 and in full view in Fig. 4.24. The GUI is used to parametrize the HEMS, letting the user input all the technical parameters of the prosumer residence, such as the EV, the home battery, the heating/cooling system, the demand response mechanism and the PV panels. Once the optimization values and the communication settings are properly configured, the user can execute the day-ahead optimization algorithm. The system set-points/outputs of the algorithm are 24h time-series that are saved and applied to the real-time circuit automatically. The GUI also features real-time tracking of electric circuit values such as voltages, currents and powers by utilizing the analog-to-digital converter chips that are provided on the microcontrollers.

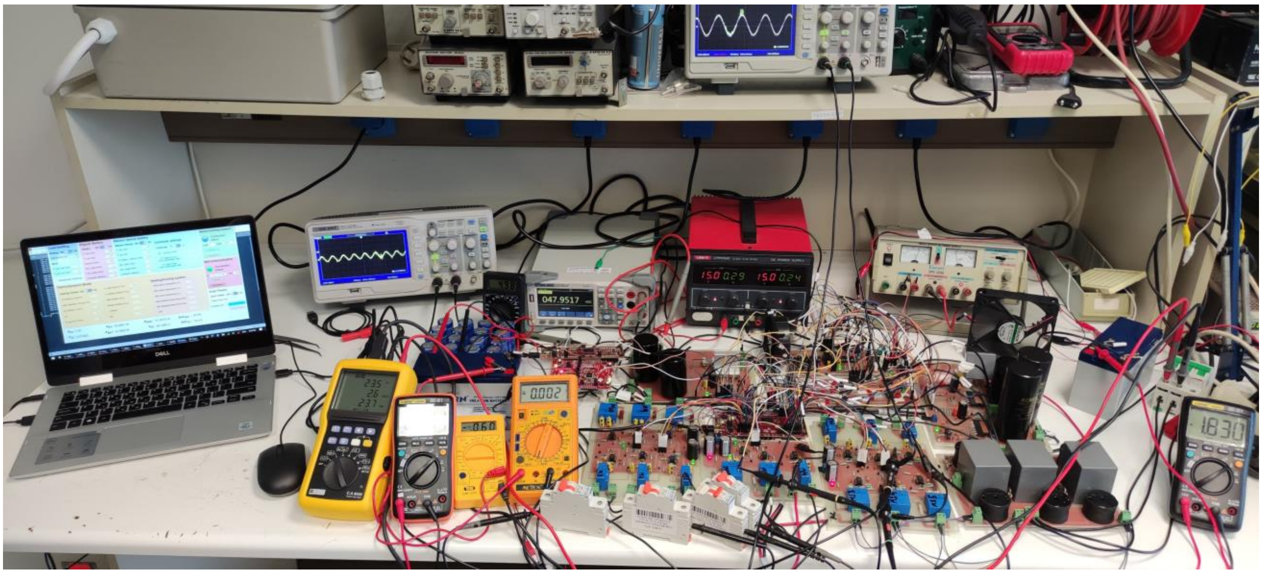

Fig. 4.23 - Experimental low-voltage prototype of the prosumer residence

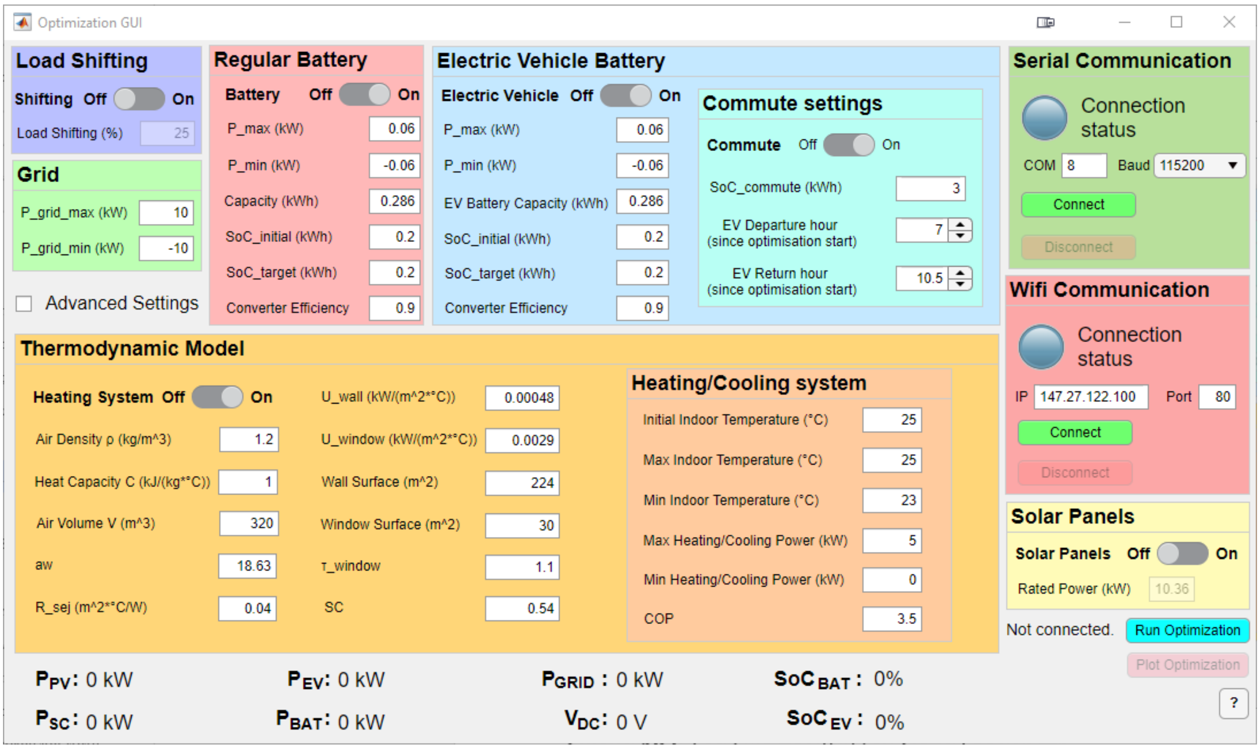

Fig. 4.24 - GUI environment for parametrizing the HEMS

5.
CONCLUSIONS

In this dissertation, an innovative multi-faceted HEMS for modern residential microgrids is proposed. The novel ideas put forth in this dissertation are the following: a) the integrated approach includes multiple energy optimization components, including flexible electric and thermal loads, EVs , ESSs and local power generation, b) the optimized provision of frequency to the grid in respect to the power components, c) the joint optimization energy costs in both grid-connected and autonomous operation while ensuring plenty of constraints and d) the development and implementation of a residential load forecasting system that combines k-means clustering and ANNs to efficiently predict the residential loads.

The PSO algorithm was implemented to solve the multi-objective power management optimization problem. Through the many simulated scenarios, the effectiveness of the HEMS in cost saving is proven, while at the same time all constraints regarding operational limits of power components and user satisfaction and comfort are satisfied. The capability of the proposed HEMS to provide frequency support while maintaining each module's flexibility to the highest possible level is also proven. Finally, through comparison of different scenarios, it is shown that cost saving of at least 25% are achievable.

6.
REFERENCES

[1] S. K. Sahoo, A. K. Sinha and N. K. Kishore, "Control Techniques in AC, DC, and Hybrid AC–DC Microgrid: A Review," *in IEEE Journal of Emerging and Selected Topics in Power Electronics,* vol. 6, no. 2, pp. 738-759, June 2018.

[2] J. P. Barton and D. G. Infield, "Energy storage and its use with intermittent renewable energy," *IEEE Transactions on Energy Conversion,* vol. 19, no. 2, pp. 441-448, June 2004.

[3] F. D. Kanellos, "Optimal Scheduling and Real-Time Operation of Distribution Networks With High Penetration of Plug-In Electric Vehicles," *IEEE Systems Journal,* vol. 15, no. 3, pp. 3938-3947, Sept 2021.

[4] J. A. P. Lopes, F. J. Soares and P. M. R. Almeida, "Integration of Electric Vehicles in the Electric Power System," *Proceedings of the IEEE,* vol. 99, no. 1, pp. 168-183, Jan 2011.

[5] M. Muratori and G. Rizzoni, "Residential Demand Response: Dynamic Energy Management and Time-Varying Electricity Pricing," *IEEE Transactions on Power Systems,* vol. 31, no. 2, pp. 1108-1117, March 2016.

[6] B. Lundstrom, S. Patel, S. Attree and M. V. Salapaka, "Fast Primary Frequency Response using Coordinated DER and Flexible Loads: Framework and Residential-scale Demonstration," *2018 IEEE Power & Energy Society General Meeting (PESGM),* pp. 1-5, 2018.

[7] I. Kalaitzakis, M. Dakanalis and F. D. Kanellos, "Optimal Power Management for Residential PEV Chargers with Frequency Support Capability," *2021 10th International Conference on Modern Circuits and Systems Technologies (MOCAST),* pp. 1-4, 2021.

[8] J. Leitão, P. Gil, B. Ribeiro and A. Cardoso, "A Survey on Home Energy Management," *IEEE Access,* vol. 8, pp. 5699-5722, 2020.

[9] U. Zafar, S. Bayhan and A. Sanfilippo, "Home Energy Management System Concepts, Configurations, and Technologies for the Smart Grid," *IEEE Access,* vol. 8, pp. 119271-119286, 2020.

[10] H. Shareef, M. S. Ahmed, A. Mohamed and E. A. Hassan, "Review on Home Energy Management System Considering Demand Responses, Smart Technologies, and Intelligent Controllers," *IEEE Access,* vol. 6, pp. 24498-24509, 2018.

[11] H. T. Dinh, J. Yun, D. M. Kim, K. -H. Lee and D. Kim, "A Home Energy Management System With Renewable Energy and Energy Storage Utilizing Main Grid and Electricity Selling," *IEEE Access,* vol. 8, pp. 49436-49450, 2020.

[12] L. Yu, W. Xie, D. Xie, Y. Zou, D. Zhang, Z. Sun, L. Zhang, Y. Zhang and T. Jiang, "Deep Reinforcement Learning for Smart Home Energy Management," *IEEE Internet of Things Journal,* vol. 7, no. 4, pp. 2751-2762, April 2020.

[13] M. Yousefi, A. Hajizadeh, M. N. Soltani and B. Hredzak, "Predictive Home Energy Management System With Photovoltaic Array, Heat Pump, and Plug-In Electric Vehicle," *IEEE Transactions on*

Industrial Informatics, vol. 17, no. 1, pp. 430-440, Jan 2021.

[14] Y. Sun, H. Yue, J. Zhang and C. Booth, "Minimization of Residential Energy Cost Considering Energy Storage System and EV With Driving Usage Probabilities," *IEEE Transactions on Sustainable Energy,* vol. 10, no. 4, pp. 1752-1763, Oct 2019.

[15] S. Rafique, M. J. Hossain, M. S. H. Nizami, U. B. Irshad and S. C. Mukhopadhyay, "Energy Management Systems for Residential Buildings With Electric Vehicles and Distributed Energy Resources," *IEEE Access,* vol. 9, pp. 46997-47007, 2021.

[16] X. Hou, J. Wang, T. Huang, T. Wang and P. Wang, "Smart Home Energy Management Optimization Method Considering Energy Storage and Electric Vehicle," *IEEE Access,* vol. 7, pp. 144010-144020, 2019.

[17] X. Wu, X. Hu, Y. Teng, S. Qian and R. Cheng, "Optimal integration of a hybrid solar-battery power source into smart home nanogrid with plug-in electric vehicle," *Journal of Power Sources,* vol. 363, pp. 277-283, 2017.

[18] L. Chandra and S. Chanana, "Energy Management of Smart Homes with Energy Storage, Rooftop PV and Electric Vehicle," *2018 IEEE International Students' Conference on Electrical, Electronics and Computer Science (SCEECS),* pp. 1-6, 2018.

[19] A. Sangswang and M. Konghirun, "Optimal Strategies in Home Energy Management System Integrating Solar Power, Energy Storage, and Vehicle-to-Grid for Grid Support and Energy Efficiency," *IEEE Transactions on Industry Applications,* vol. 56, no. 5, pp. 5716-5728, Sept.-Oct. 2020.

[20] X. Xu, Y. Jia, Y. Xu, Z. Xu, S. Chai and C. S. Lai, "A Multi-Agent Reinforcement Learning-Based Data-Driven Method for Home Energy Management," *IEEE Transactions on Smart Grid,* vol. 11, no. 4, pp. 3201-3211, July 2020.

[21] H. T. Dinh and D. Kim, "An Optimal Energy-Saving Home Energy Management Supporting User Comfort and Electricity Selling With Different Prices," *IEEE Access,* vol. 9, pp. 9235-9249, 2021.

[22] R. Faia, P. Faria, Z. Vale and J. Spinola, "Demand Response Optimization Using Particle Swarm Algorithm Considering Optimum Battery Energy Storage Schedule in a Residential House," *Energies,* vol. 12, no. 9, p. 1645, April 2019.

[23] A. Imran, G. Hafeez, I. Khan, M. Usman, Z. Shafiq, A. B. Qazi, A. Khalid and K. -D. Thoben, "Heuristic-Based Programable Controller for Efficient Energy Management Under Renewable Energy Sources and Energy Storage System in Smart Grid," *IEEE Access,* vol. 8, pp. 139587-139608, 2020.

[24] S. M. Hosseini, R. Carli and M. Dotoli, "Robust Optimal Energy Management of a Residential Microgrid Under Uncertainties on Demand and Renewable Power Generation," *IEEE Transactions on Automation Science and Engineering,* vol. 18, no. 2, pp. 618-637, April 2021.

[25] H. Golpîra and S. Khan, "A multi-objective risk-based robust optimization approach to energy management in smart residential buildings under combined demand and supply uncertainty," *Energy,* vol. 170, pp. 1113-1129, 2019.

[26] X. Jin, J. Wu, Y. Mu, M. Wang, X. Xu and J. Hongjie, "Hierarchical microgrid energy management in an office building," *Applied Energy,* vol. 208, pp. 480-494, 2017.

[27] G. K. Farinis and F. D. Kanellos, "Integrated energy management system for Microgrids of building prosumers," *Electric Power Systems Research,* vol. 198, p. 107357, 2021.

[28] J. Duffie and W. Beckman, Solar engineering of thermal process, New York: Wiley, 1991.

[29] F. D. Kanellos, K. Kalaitzakis, I. Psarras and Y. Katsigiannis, "Efficient and robust power and energy management for large clusters of plug-in electric vehicles and distribution networks," *IET Energy Systems Integration,* pp. 1-16, April 2022.

[30] Shirazi, Yosef & Carr, Edward & Knapp, Lauren. (2015). A cost-benefit analysis of alternatively

fueled buses with special considerations for V2G technology. Energy Policy. 87. 591-603. 10.1016/j.enpol.2015.09.038.

[31] Zachary Shahan, 2016, “Tesla CTO JB Straubel On Why EVs Selling Electricity To The Grid Is Not As Swell As It Sounds”, https://cleantechnica.com/2016/08/22/vehicle-to-grid-used-ev-batteries-grid-storage/

[32] Uddin, Kotub; Jackson, Tim; Widanage, Widanalage D.; Chouchelamane, Gael; Jennings, Paul A.; Marco, James (August 2017). "On the possibility of extending the lifetime of lithium-ion batteries through optimal V2G facilitated by an integrated vehicle and smart-grid system". Energy. 133: 710–722. doi:10.1016/j.energy.2017.04.116

[33] Katiraei, F. & Iravani, Reza & Hatziargyriou, Nikos & Dimeas, Aris. (2008). Microgrids Management. Power and Energy Magazine, IEEE. 6. 54 - 65. 10.1109/MPE.2008.918702.

[34] Suyanto, Heri & Rina, Irawati. (2017). Study trends and challenges of the development of microgrids. 383-387. 10.1109/QIR.2017.8168516.

[35] Chenghua Zhang, Jianzhong Wu, Yue Zhou, Meng Cheng, Chao Long,Peer-to-Peer energy trading in a Microgrid,Applied Energy,Volume 220,2018,Pages 1-12,ISSN 0306-2619,https://doi.org/10.1016/j.apenergy.2018.03.010.

[36] D. E. Olivares *et al*., "Trends in Microgrid Control," in *IEEE Transactions on Smart Grid*, vol. 5, no. 4, pp. 1905-1919, July 2014, doi: 10.1109/TSG.2013.2295514.

[37] K. Strunz, E. Abbasi and D. N. Huu, "DC Microgrid for Wind and Solar Power Integration," in *IEEE Journal of Emerging and Selected Topics in Power Electronics*, vol. 2, no. 1, pp. 115-126, March 2014, doi: 10.1109/JESTPE.2013.2294738.

[38] S. Parhizi, H. Lotfi, A. Khodaei and S. Bahramirad, "State of the Art in Research on Microgrids: A Review," in *IEEE Access*, vol. 3, pp. 890-925, 2015, doi: 10.1109/ACCESS.2015.2443119.

[39] T. Kim, A. Stoica, and R.-S. Chang, Eds., “Security-Enriched Urban Computing and Smart Grid,” Communications in Computer and Information Science, 2010.

[40] Saleh, M.; Esa, Y.; Mhandi, Y.; Brandauer, W.; Mohamed, A. (October 2016). "Design and implementation of CCNY DC microgrid testbed". 2016 IEEE Industry Applications Society Annual Meeting: 1–7. doi:10.1109/IAS.2016.7731870. ISBN 978-1-4799-8397-1.

[41] Uddin, Kotub; Dubarry, Matthieu; Glick, Mark B. (February 2018). "The viability of vehicle-to-grid operations from a battery technology and policy perspective". Energy Policy. 113: 342–347. doi:10.1016/j.enpol.2017.11.015.

[42] Paulraj, Pon (2019-12-10). "What is V1G, V2G and V2H / V2B / V2X? | Integrating electric vehicles into power grid" https://www.emobilitysimplified.com/2019/12/what-is-vehicle-to-grid-v1g-v2g-v2x-v2h.html

[43] Shen, Jingshuang & Jiang, Chuanwen & Li, Bosong. (2015). Controllable Load Management Approaches in Smart Grids. Energies. 8. 11187-11202. 10.3390/en81011187.

[44] Liasi, Sahand Ghaseminejad; Bathaee, Seyed Mohammad Taghi (2017). "Optimizing microgrid using demand response and electric vehicles connection to microgrid". 2017 Smart Grid Conference (SGC). pp. 1–7. doi:10.1109/SGC.2017.8308873. ISBN 978-1-5386-4279-5.

[45] Considine, Toby & Cox, William. (2009). Smart Loads and Smart Grids—Creating the Smart Grid Business Case. 10.13140/2.1.1092.3200.

[46] M. Nemati, S. Tenbohlen, M. Imran, H. Mueller and M. Braun, "Frequency and voltage control in microgrids: Modeling and simulations in islanded mode," *IEEE PES Innovative Smart Grid Technologies, Europe*, Istanbul, 2014, pp. 1-6, doi: 10.1109/ISGTEurope.2014.7028858.

[47] Zhou, XueSong & Guo, Tie & Ma, YouJie. (2017). An Overview on Operation and Control of Microgrid. DEStech Transactions on Engineering and Technology Research. 10.12783/dtetr/mcee2016/6412.

[48] Chen, Min-Rong & Wang, Huan & Zeng, Guo-Qiang & Dai, Yu-Xing & Bi, Da-Qiang. (2018). Optimal P-Q Control of Grid-Connected Inverters in a Microgrid Based on Adaptive Population Extremal Optimization. Energies. 11. 2107. 10.3390/en11082107.

[49] Amicarelli, Elvira & Tran-Quoc, T. & Seddik, Bacha. (2017). Optimization algorithm for microgrids day-ahead scheduling and aggregator proposal. 1-6. 10.1109/EEEIC.2017.7977487.

[50] Allruwaili, Ali Barjs, "The Impact of Different Battery Technologies for Remote Microgrids" (2016). Theses and Dissertations. 1071. http://openprairie.sdstate.edu/etd/1071

[51] U.S. Department of Energy, 2013, “Grid Energy Storage”, https://www.energy.gov/sites/prod/files/2014/09/f18/Grid%20Energy%20Storage%20December%202013.pdf

[52] Palizban, Omid; Kauhaniemi, Kimmo (May 2016). "Energy storage systems in modern grids—Matrix of technologies and applications". Journal of Energy Storage. 6: 248–259. doi:10.1016/j.est.2016.02.001.

[53] David Roberts, 2019, “Getting to 100% renewables requires cheap energy storage. But how cheap?”, https://www.vox.com/energy-and-environment/2019/8/9/20767886/renewable-energy-storage-cost-electricity

[54] Rehman, Shafiqur; Al-Hadhrami, Luai; Alam, Md (30 April 2015). "Pumped hydro energy storage system: A technological review". Renewable and Sustainable Energy Reviews. 44: 586–598. doi:10.1016/j.rser.2014.12.040

[55] Ma, Zhiwen, Josh Eichman, and Jennifer Kurtz. 2018. “Fuel Cell Backup Power System for Grid Service and Micro-Grid in Telecommunication Applications: Preprint.” Golden, CO: National Renewable Energy Laboratory. NREL/CP-5500-70990. URL. https://www.nrel.gov/docs/fy18osti/70990.pdf

[56] Qiao-Chu He, Yun Yang, Lingquan Bai, Baosen Zhang,Smart energy storage management via information systems design,Energy Economics,Volume 85,2020,104542,ISSN 0140-9883,https://doi.org/10.1016/j.eneco.2019.104542.

[57] Hua, Y.; Shentu, X.; Xie, Q.; Ding, Y. Voltage/Frequency Deviations Control via Distributed Battery Energy Storage System Considering State of Charge. Appl. Sci. 2019, 9, 1148.

[58] Center for Sustainable Systems, University of Michigan, 2019, “U.S. GRID ENERGY STORAGE FACTSHEET”, http://css.umich.edu/factsheets/us-grid-energy-storage-factsheet

[59] Aluisio, B.; Bruno, S.; De Bellis, L.; Dicorato, M.; Forte, G.; Trovato, M. DC-Microgrid Operation Planning for an Electric Vehicle Supply Infrastructure. Appl. Sci. 2019, 9, 2687.

[60] Ebrahim Mortaz, Jorge Valenzuela,Microgrid energy scheduling using storage from electric vehicles,Electric Power Systems Research,Volume 143,2017,Pages 554-562,ISSN 0378-7796,https://doi.org/10.1016/j.epsr.2016.10.062.

[61] Mark Goody, 2019, “The role of electric vehicles in a microgrid before V2G”, https://www.fleetcarma.com/microgrids-and-v2g/

[62] de Dear, R., & Brager, G. (1998). Developing an adaptive model of thermal comfort and preference. UC Berkeley: Center for the Built Environment. Retrieved from https://escholarship.org/uc/item/4qq2p9c6

[63] Chenghua Zhang, Jianzhong Wu, Yue Zhou, Meng Cheng, Chao Long,Peer-to-Peer energy trading in a Microgrid,Applied Energy,Volume 220,2018,Pages 1-12,ISSN 0306-2619,https://doi.org/10.1016/j.apenergy.2018.03.010.

[64] Thavlov, A., & Bindner, H. W. (2012). Thermal Models for Intelligent Heating of Buildings. In Proceedings of the International Conference on Applied Energy, ICAE 2012 (pp. A10591)

[65] Li, Zhengmao & Xu, Yan. (2019). Temporally-coordinated optimal operation of a multi-energy microgrid under diverse uncertainties. Applied Energy. 240. 719-729. 10.1016/j.apenergy.2019.02.085.

[66] California Public Utilities Commission, 2017, "Southern California Edison Company's Department of Defense Vehicle-to-Grid Final Report", http://www.cpuc.ca.gov/WorkArea/DownloadAsset.aspx?id=6442455793

[67] Du, Ruoyang; Robertson, Paul (2017). "Cost Effective Grid-Connected Inverter for a Micro Combined Heat and Power System". IEEE Transactions on Industrial Electronics. 64 (7): 5360–

5367. doi:10.1109/TIE.2017.2677340.

[68] Jon Porter, 2019, “Fake noise will be added to new electric cars starting today in the EU”, https://www.theverge.com/2019/7/1/20676854/electric-cars-artificial-safety-noise-low-speeds-european-union-rules-2019-2021

[69] Dei.gr, Two-zone power tariff timetables, https://www.dei.gr/el/oikiakoi-pelates/timologia-mar262020/oikiako-timologio-me-xronoxrewsi-oikiako-nuxterinoMar26202070230690PM/wrarioMar26202070231340PM

[70] Dei.gr, Two-zone power tariff cost tables, https://www.dei.gr/Documents2/TIMOLOGIA/%CE%A4%CE%99%CE%9C-30-6-2020/TIMOK-XT-2020-G1N-JUN20(3%CF%80%CE%BB%CE%BF).pdf

[71] Α. Ματωνάκη, Κ. Καλύμνιος, «Μεθοδολογία Δημιουργίας Τυπικών Διαγραμμάτων Φορτίου για Οικιακούς Καταναλωτές», ΑΠΘ, Θεσσαλονίκη, Μάρτιος 2009